Lawrence Berkeley National Laboratory

Title
Fine-tuning of canted magnetization in stepped Fe films through thickness variation, Au capping, and quantum confinement

Permalink
https://escholarship.org/uc/item/779734bm

Journal
Physical Review B, 99(18)

ISSN
2469-9950

Authors
Dąbrowski, M
Cinal, M
Schmid, AK
et al.

Publication Date
2019-05-01

DOI
10.1103/physrevb.99.184420

Peer reviewed

Fine tuning of canted magnetization in stepped Fe films through thickness variation, Au capping and quantum confinement

M. Dąbrowski,[1,2] M. Cinal,[3] A. K. Schmid,[4] J. Kirschner,[1,5] and M. Przybylski[1,6]

[1]*Max-Planck-Institut für Mikrostrukturphysik, 06120 Halle, Germany*
[2]*Department of Physics and Astronomy, University of Exeter, Exeter EX4 4QL, UK*
[3]*Institute of Physical Chemistry of the Polish Academy of Sciences, 01-224 Warsaw, Poland*
NCEM, Molecular Foundry, Lawrence Berkeley National Laboratory, Berkeley, California 94720, USA
[5]*Naturwissenschaftliche Fakultät II, Martin-Luther-Universität Halle-Wittenberg, 06120 Halle, Germany*
[6]*Faculty of Physics and Applied Computer Science,*
AGH University of Science and Technology, 30-059 Kraków, Poland
(Dated: January 29, 2019)

We present a joint experimental and theoretical study that demonstrates how to efficiently control a canted state of magnetization in Fe films grown on Ag(001) vicinal surface and precisely characterize it with the magneto-optical Kerr effect. It is shown that by employing different mechanisms to tune the magnetization tilting angle, any magnetization orientation within the plane perpendicular to the step edges can be achieved. In particular, increasing the Fe film thickness leads to continuous rotation of the magnetization easy axis towards the film surface and the sense of this rotation in uncovered films is opposite to that in films covered with Au. Another tuning mechanism is provided by oscillatory changes of the tilting angle at low temperatures due to formation of quantum well states in Fe films. The observed canting of magnetization is explained within a phenomenological model by an interplay of the shape anisotropy and two magnetocrystalline anisotropy terms, perpendicular and step-induced anisotropies, which results in an effective uniaxial magnetic anisotropy. The fitted thickness dependencies of the anisotropy constants accurately reproduce experimental variations of the tilting angle with both Fe and Au thicknesses as well as transient changes of the magnetization orientation in ultrathin Fe films upon sub-monolayer Au coverage, observed with spin-polarized low energy electron microscopy.

PACS numbers:

I. INTRODUCTION

Demand for faster, smaller and low power consumption data storage has fueled efforts to find alternative ways to store magnetic bits[1–3]. In the case of ferromagnetic transition metals, voltage pulses[4,5], microwaves[6] and optical pulses[7–9] are arguably the most promising methods to control the orientation of the magnetization. In all three types of the excitations, a canted state of the magnetization is often desirable in order to increase a torque on the magnetization vector[5,8,10]. A canted state is usually achieved via an external magnetic field[5], interlayer exchange coupling[11] or an appropriate choice of a ferromagnetic film (and its thickness), in which a spin reorientation transition (SRT) from in-plane to out-of-plane orientation occurs[12]. The latter method is in general the most straightforward, since it does not require an external field and additional coupling layers. In practice however, the SRT thickness range is rather narrow and dependent on even tiny changes in magnetic anisotropy (which can be affected by many factors such as temperature, preparation conditions, capping layers etc.). In this context, ferromagnetic films grown on vicinal surfaces are advantageous, because they allow for observing a canted magnetization in wider thickness range and with well defined magnetization inclination direction as shown for Ni[13,14], Co[15] and Fe[16].

Here we focus on Fe thin films grown on the Ag(116) vicinal surface, where a canted magnetization state extends over a wide Fe thickness range and is characterized by stripe domains with domain walls oriented perpendicular to the steps[16]. Upon increasing the Fe film thickness the magnetization rotates continuously from the direction perpendicular to the terraces plane towards the sample plane and switches the in-plane component abruptly to the direction parallel to the step edges only when the canting becomes small and the magnetization is oriented nearly exactly in the sample plane[16]. The rotation of the magnetization is confined to the plane perpendicular to the step edges. This allows us to employ magneto-optical Kerr effect (MOKE) in longitudinal geometry, where both polar and longitudinal MOKE signals can be probed and the tilting angle of the magnetization δ can be precisely extracted[17]. We show that the canted magnetization can be controlled with high accuracy by changing the thickness of either the Fe film or the Au capping layer. In particular, we demonstrate that covering the Fe film with Au affects the magnetization rotation direction and allows to reverse the sense of rotation.

An additional degree of freedom in the manipulation of the canted magnetization state is achieved by cooling the sample down to 5 K. At lower temperature the SRT thickness range is broadened due to changed thickness dependence of magnetic anisotropy[18]. In consequence, virtually any magnetization orientation within the plane perpendicular to the steps can be achieved by appropriate choice of Fe and Au thicknesses. Furthermore, the

measurements at 5 K allow to explore the effect of quantum well states (QWS) on the magnetic anisotropy of our system. While there have been several reports on QWS driven magnetic anisotropy changes with the easy axis of the magnetization in the sample plane[19–22], the experiments on perpendicular magnetic anisotropy are sparse, and concern solely slightly tilted magnetization[17]. Here we show that QWS lead to periodic changes of canted magnetization and significantly modify the SRT process for both uncovered and Au-covered Fe thin films.

Our experimental observations are elucidated within a phenomenological model of magnetic anisotropy in ferromagnetic films with the symmetry reduced by steps. We show that tilting of magnetization with respect to the film plane originates from the superposition of the shape anisotropy and magnetocrystalline anisotropies due to film surface/interface and steps, which is described by an effective uniaxial anisotropy within the plane perpendicular to the steps. The model predicts that the magnetization tilting angle can attain any value resulting from the relative strengths of the three anisotropy terms. By fitting the thickness dependencies of the respective anisotropy constants we are able to reproduce the observed changes of the tilting angle which are driven by variations of Fe and Au thicknesses, and d-band QWS at low temperature.

II. EXPERIMENTAL RESULTS: MOKE FOR Fe FILMS ON STEPPED Ag(001) SUBSTRATE

A. Experimental details

The experiments were performed in a multi-chamber ultrahigh vacuum system with the pressure below $2x10^{-10}$ mbar during deposition. An Ag(116) vicinal crystal [13.3° off the (001) surface] with the step edges oriented along the [$\bar{1}$10] direction was used. The Ag(116) surface was cleaned by cycles of Ar ion sputtering at 1 keV and annealing at ~775 K. Such preparation procedure yields vicinal surface characterized by regular monoatomic steps with an average terrace width of 0.86 nm, as confirmed by sharp double-split diffraction spots observed in low energy electron diffraction (LEED). Note that a perfect epitaxial growth proceeds by matching the [100] direction of a Fe film with the [110] direction of the Ag substrate. The Fe films were grown at room temperature (RT) by molecular beam epitaxy (MBE). After growth, the films were warmed up to 450 K in order to improve the surface morphology[23]. The Fe films were grown as wedge samples with a slopes of 1 ML/mm. The Au capping layers were grown by MBE at RT.

Magnetic hysteresis loops were probed by *in situ* longitudinal MOKE using *s*-polarized light with wavelength 670 nm and beam diameter <0.2 mm, incident at 30° with respect to the sample normal. The magnetic field was applied in plane, either parallel or perpendicular to the steps. Thickness dependent Kerr ellipticity measure-

ments were performed by moving the sample across the wedge at fixed laser beam position.

The domain structure of Au/Fe/Ag(116) was imaged by using spin-polarized low energy microscopy (SPLEEM)[24,25]. Three components of the magnetization vector M_x, M_y and M_z were probed by measuring the magnetic contrast in three orthogonal spin-polarizations of the incident beam. For detailed description of SPLEEM experiment we refer to[25,26].

B. Hysteresis loops for Fe films on vicinal surfaces

Epitaxial growth of Fe films on vicinal Ag(001) substrates results in additional contributions to magnetic anisotropy, especially, in a step-induced uniaxial anisotropy with the easy magnetization axis oriented along or perpendicular to the step edges[18]. In the case of a thick Fe film with an in-plane magnetization, the easy axes of the four-fold anisotropy of the Fe film are oriented along and perpendicular to the step edges. One of them becomes the easy magnetization axis and the other the intermediate magnetization axis due to uniaxial in-plane anisotropy induced by steps. This results in split hysteresis loops, when the magnetic field is applied along intermediate axis (i.e., perpendicular to the easy axis in the sample plane). Split hysteresis loops are characterized by a shift field H_s, which is a measure of the step-induced in-plane uniaxial anisotropy. With decreasing Fe film thickness, an uniaxial magnetocrystalline anisotropy favoring perpendicular orientation of the magnetization along [001] direction, becomes comparable to a shape anisotropy favoring in-plane orientation. As a consequence of the competition between these two anisotropies, the magnetization is tilted within the plane perpendicular to the steps[16]. By measuring the magneto-optical Kerr signal in the longitudinal configuration and with the field applied perpendicular to the steps, even tiny changes of the tilting angle δ can be observed, as it has been shown previously for nearly in-plane magnetized Co[20,27,28] and Fe[17] films.

In order to probe the orientation of tilted magnetization, in the first step the measurements were done in a configuration α^+, with the magnetic field and the laser beam oriented as it is shown in Fig. 1(a),(b). The Kerr ellipticity of the measured hysteresis loop in α^+ geometry, $\phi_{\alpha+}^H$, comprises both the longitudinal ϕ_L and the polar ϕ_P Kerr ellipticities. Polar Kerr signal ϕ_P contributes to the total Kerr signal due to a component of the magnetization normal to the film plane which exists in the case the magnetization is tilted out of the sample plane. If the normal magnetization component is pointing outwards from the film surface the polar Kerr ellipticity ϕ_P is positive (for the laser beam with the *s* polarization) and changes to negative for the opposite direction of that magnetization component. Since the polar Kerr effect is much stronger than the longitudinal Kerr effect[29], the polar term of the total Kerr ellipticity
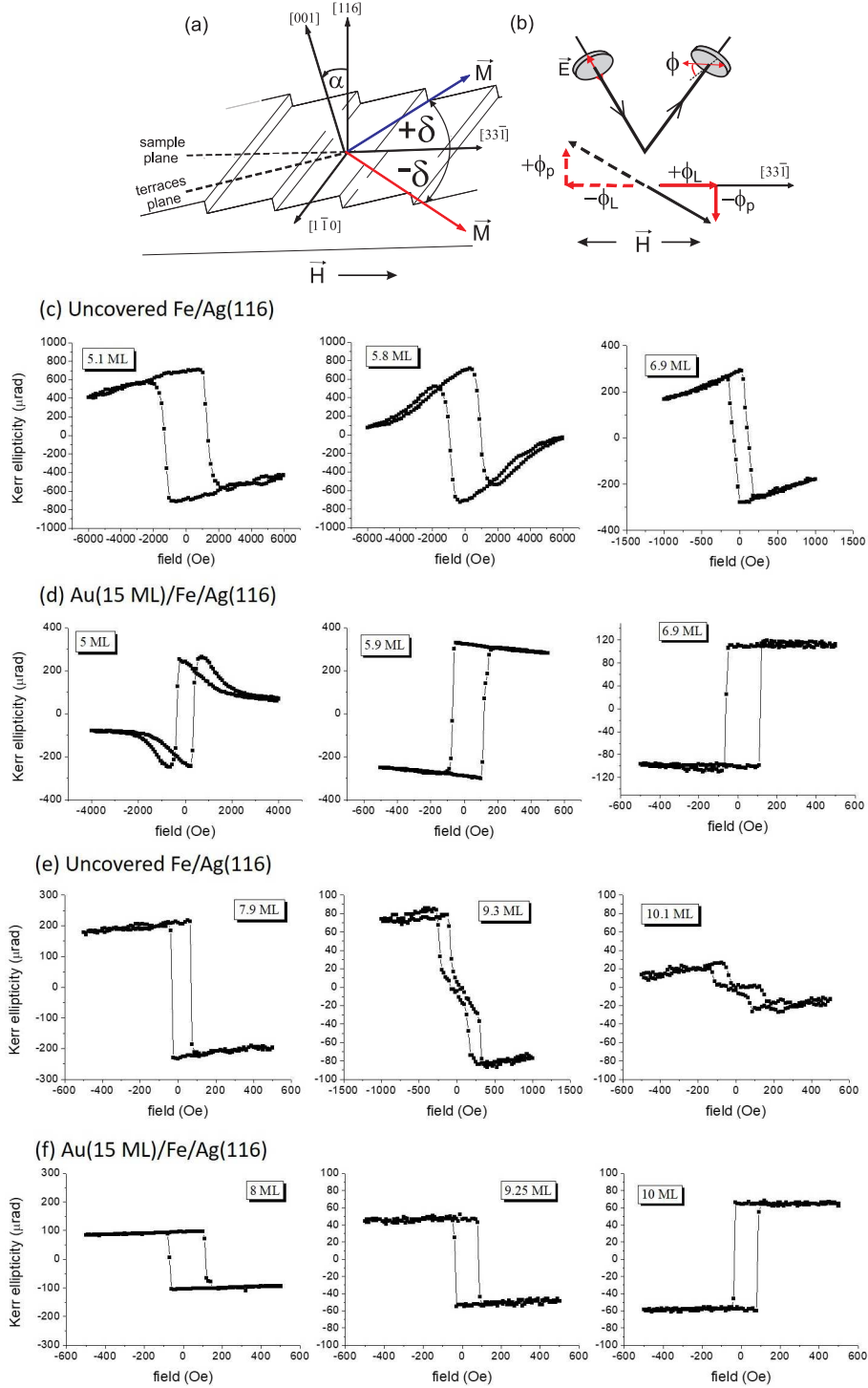
FIG. 1: (a) Crystallographic directions and corresponding possible canted magnetization orientations within the plane perpendicular to the steps for FM film on the (116) vicinal surface. Magnetization vectors with positive and negative tilting angles are shown by blue and red arrow, respectively. The miscut angle α defines the angle between the sample plane and terraces plane and for our Ag(116) surface is equal to 13.3^o. (b) Schematics of LMOKE measurement and LMOKE signal decomposition into longitudinal (ϕ_L) and polar (ϕ_P) components (for clarity, only the case of negative tilting angle is shown). The geometry of LMOKE with the light incident from the left with respect to the terraces orientation as in (a) is defined as α^+ geometry. Hysteresis loops measured at α^+ geometry at $T = 5$ K for uncovered (c),(e) and covered with Au (d),(f) Fe films with different thicknesses.
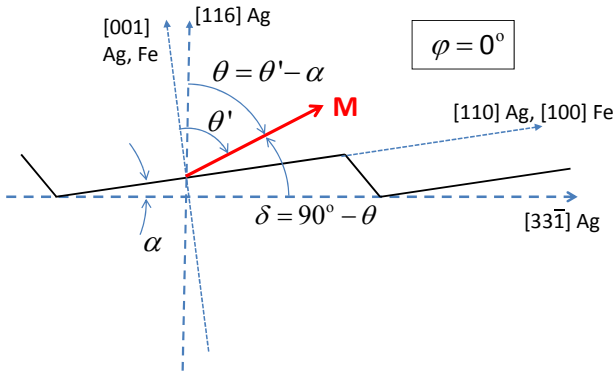
FIG. 2: Magnetization orientation characterized (equivalently) by the angles δ, θ and θ' within the plane perpendicular to the steps for a Fe film on the Ag(116) surface with the vicinal angle $\alpha = 13.3°$.

$\phi_{\alpha+}^H = \phi_L + \phi_P$ dominates and determines the sign of $\phi_{\alpha+}^H$, unless the polar term is small.

The measured hysteresis loops change substantially while varying the thickness of both Fe film and Au overlayer. In particular, reversed square loops are found for uncovered Fe films with the thickness from 5.1 to 6.9 ML [Fig. 1(c)] and square loops are obtained if these films are covered with Au [Fig. 1(d)] (where by a reverse loop we mean positive Kerr signal at negative magnetic field and negative negative Kerr signal at positive magnetic field). As a result, the MOKE signal $\phi_{\alpha+}^H$ at remanence is negative for the uncovered films and becomes positive upon their coverage with Au, which corresponds to changing direction of the normal magnetization component. A square hysteresis loop, is also found for the Fe(7.9 ML) film, but with a further increase of the Fe thickness it changes to the split hysteresis loop, indicating a spin reorientation transition (SRT) to the magnetization direction parallel to the steps [Fig. 1(e)].

Such SRT is not observed in the MOKE results shown in Fig. 1(f) for Au-covered Fe films with thicknesses up to 10 ML. However, the square loops are found to be reversed upon changing the Fe thickness from below 6.9 ML to 8.0 and 9.25 ML, thus attaining similar shape to uncovered Fe films, while further increasing the Fe thickness to 10 ML for the Au-covered Fe films retains the original loop character found for the Au-covered films with the thickness of 6.9 ML or thinner. This indicates that the normal component of magnetization at remanence switches direction with increasing Fe thickness in the case of the Au-covered films. Here, we refer to the remanent magnetic state for both uncovered and Au-covered Fe films obtained by switching off a positive magnetic field applied perpendicular to the steps along the $[33\bar{1}]$ axis .

The hysteresis loops for the magnetization perpendicular to the steps are not strictly square. This is because the magnetic field applied in-plane perpendicular to the steps is not oriented along the easy axis which is tilted away from the film plane. Thus, the measured Kerr signal

decreases with increasing magnetic field due to decreasing polar Kerr signal ϕ_P (as a result of decreasing the normal component of the magnetization which is forced by the field to rotate from the easy axis towards the field direction in the surface plane).

To understand the observed changes of magnetization direction with increasing thickness of the Fe films and/or with covering by Au, the following model of the magnetic anisotropy of ferromagnetic films on vicinal surfaces has been developed.

III. MAGNETIC ANISOTROPY OF Fe FILMS ON STEPPED SUBSTRATES -PHENOMENOLOGICAL MODEL

A. Model - general

The orientation of magnetization is characterized by the polar angle θ measured from the normal to the macroscopic film surface (i.e., the sample plane) and the azimuthal angle φ measured with respect to the in-plane direction perpendicular to the step edges; Equivalently, the tilting angle:

$$\delta = 90° - \theta \qquad (1)$$

measured with respect to the sample plane can be used instead of θ for magnetization perpendicular to the steps; see Fig. 2.

The total energy of a ferromagnetic film deposited on the stepped substrate depends on direction of magnetization **M** as follows:

$$
\begin{aligned}
E(\theta, \varphi) &= K_{\text{dip}} \cos^2 \theta + K_s \sin^2 \theta' - K_u \sin^2 \theta' \sin^2 \varphi' \\
&\quad - \frac{1}{2} K_{\text{sp}} \sin 2\theta' \cos \varphi' + E_{\text{bulk}}(\theta', \varphi') \\
&\equiv K_{\text{dip}} \cos^2 \theta + E_{\text{MCA}} .
\end{aligned} \qquad (2)
$$

which agrees with the formula used by Kawakami *et al.*[18] The shape anisotropy depends on the polar angle θ and the respective anisotropy constant $K_{\text{dip}} = 2\pi M^2 t_{\text{FM}}$ increases linearly with the film thickness t_{FM} (if the film energy is calculated per unit area of the film surface). The magnetocrystalline anisotropy (MCA) energy E_{MCA} arising from the spin-orbit interaction (treated as a perturbation in the Hamiltonian) comprises three second-order contributions with the angular dependences shown in Eq. (2) and the fourth-order bulk contribution E_{bulk}.

The MCA energy depends on the angles θ' and φ' describing magnetization orientation with respect to the main crystallographic axes of the bcc Fe films. The angle θ' is measured with respect to the [001] axis, while φ' is measured – in the terrace plane (001) – with respect to the [100] axis of the Fe film, which is perpendicular to the steps and equivalent to the [110] axis of the Ag substrate. If magnetization **M** is perpendicular to the steps and shows positive longitudinal component (i.e, $\varphi = \varphi' = 0$),

as in remanence in the α^+ configuration, we obtain:

$$\theta' = \theta + \alpha \qquad (3)$$

where α denotes vicinal angle. For magnetization parallel to the steps (i.e., at $\varphi' = \varphi = 90°$) the two polar angles are equal: $\theta' = \theta$.

The angular dependence of the second-order contribution to the MCA energy includes three anisotropy constants K_s, K_{sp}, and K_u. They can be expressed by the following energy differences:

$$K_s \;=\; E_{MCA}(100) - E_{MCA}(001) \qquad (4)$$
$$K_u \;=\; E_{MCA}(100) - E_{MCA}(010) \qquad (5)$$
$$K_{sp} \;=\; E_{MCA}(10\overline{1}) - E_{MCA}(101)\,. \qquad (6)$$

defined with the MCA energy $E_{MCA}(hkl)$ for different orientations $[hkl]$ of magnetization which are not equivalent for the film on a stepped substrate. These directions are oriented along the following cubic symmetry axes of the bcc Fe: [001] ($\theta' = 0°$, perpendicular to the terrace surface), [010] ($\theta' = 90°, \varphi' = 90°$, parallel to the steps), [100] ($\theta' = 90°, \varphi' = 0°$, perpendicular to the steps within the terrace plane), [101] ($\theta' = 45°, \varphi' = 0°$), and [10$\overline{1}$] ($\theta' = -45°, \varphi' = 0°$).

Thus, the uniaxial perpendicular anisotropy constant K_s originates from the film's interface, similarly to flat films[18]. The remaining two anisotropy constants K_u and K_{sp} arise from the steps of the vicinal surface and both vanish for flat films with a cubic crystal structure and the (001) surface. The phenomenological Néel's model, based on anisotropy contributions from pairs of the first-nearest neighbours, predicts $K_u = 0$ for films with bcc lattice and steps along the [010] axis.[18] However, this anisotropy constant is not expected to vanish completely in a more accurate quantum-mechanical approach[30] since the four-fold in-plane symmetry is broken in films grown on stepped substrates. Therefore, we allow for a finite value of K_u, though it is presumably much smaller than the other step-induced anisotropy constant K_{sp} for the considered bcc films.

The bulk anisotropy energy of a cubic crystal depends on the magnetization orientation as follows:

$$E_{bulk} = \frac{1}{4}K_b \sin^2 2\theta' + \frac{1}{4}K_b \sin^4 \theta' \sin^2 2\varphi'; \qquad (7)$$

Note that this dependence is different from but equivalent to the expression used Ref.[27] for stepped fcc films with φ' measured from the axis [110]. Since we consider the energy per unit area of the surface (or suface atom) the magnitude of the bulk anisotropy constant K_b depends linearly on the film thickness. Thus, the experimental value 4.7×10^5 erg/cm^3 of the anisotropy constant for bulk Fe[31] results in $K_b = 0.0035 \times N_{Fe}$ meV/(surface atom), where N_{Fe} denotes the number of MLs in a Fe film. For Fe films on Ag(001) substrate, the values of K_b are different for in-plane and out-of-plane directions of magnetization[32,33] (and the dependence of E_{bulk} on

the magnetization orientation is modified accordingly), however the reported values of K_b are of the same order as for bulk Fe. Thus, the variation of the bulk anisotropy energy, given by $K_b/4$ (see Eq. (7)) is less than 0.01 and 0.02 meV/(surface atom) for $N_{Fe} = 10$ and 20 ML, respectively. Therefore, it can be neglected in comparison with K_s and K_{sp}, which are a few tens times larger[16]. In particular, we neglect E_{bulk} in calculations of the tilting angle.

The bulk anisotropy can lead to a canted magnetization in flat cubic films by competing with the effective uniaxial (perpendicular) anisotropy $K_{dip} - K_s$ close to SRT[34,35]. However, such canting occurs only for negative values of K_b which is not the case for (001) Fe films thicker than 4.5 ML[36]. Even if a negative K_b of a magnitude comparable to that of bulk Fe was assumed the magnetization canting would be present only in the small interval of the film thickness where $K_{dip} - K_s$ changes from $-K_b$ to K_b. The width of this interval defines the SRT thickness range of $2K_b/k_{dip}$ and is estimated to be 0.3 ML using the shape anisotropy k_{dip} per 1 ML equal to 0.142 eV/(surface atom), which corresponds to the saturation magnetization of $M = 1725$ emu/cm^3 in bulk Fe. This SRT thickness range is around 10 times smaller than the width of the actual thickness interval (around 3 ML) in which SRT takes places in the investigated Fe films on the vicinal (116) Ag substrate (see Sec. IV). Thus, it is expected that the bulk anisotropy is not a major factor in the mechanism of magnetization canting in stepped Fe films, which provides another argument for neglecting it in the present model.

B.   Magnetization tilt

The model predicts[37] that the magnetization orientation, corresponding to the minimum of the energy $E(\theta, \varphi)$ with $E_{bulk} = 0$, is either along the steps ($\varphi = 0$) or in the vertical plane perpendicular to the steps ($\varphi = 0$ or $\varphi = 180°$), in agreement with SPLEEM experiment[16]. In the latter case the magnetization vector $\mathbf{M}$ is tilted from the terrace plane as well as from the macroscopic film surface as it is found experimentally. The value of the tilting angle (measured from the macroscopic film surface)

$$\delta = 90° - \theta_0 = 90° - \theta'_0 + \alpha \qquad (8)$$

is obtained by minimizing the total energy

$$E_\perp(\theta') = E(\theta', \varphi' = 0°) =$$
$$K_{dip}\cos^2\theta + K_s \sin^2\theta' - \frac{1}{2}K_{sp}\sin 2\theta'\,. \qquad (9)$$

obtained with $E_{bulk} = 0$ for magnetization oriented perpendicular to the steps, i.e., at $\varphi = \varphi' = 0°$. The expression for $E_\perp(\theta')$ is valid also for the extended range of $\theta' > 180°$ which corresponds to the polar angle $360° - \theta' < 180°$ and the azimuthal angle $\varphi' = 180°$ in the standard definition of these angles.

The necessary minimum condition $\partial E_\perp(\theta')/\partial\theta' = 0$ yields the analytical solution for the optimal angle $\theta' = \theta'_0$,

$$\tan 2\theta'_0 = \tan 2\alpha \, \frac{\widetilde{K}_{\rm dip} - k_{\rm sp}}{\widetilde{K}_{\rm dip} - K_{\rm s}}\,, \qquad (10)$$

which includes the scaled anisotropy constants

$$\widetilde{K}_{\rm dip} = K_{\rm dip} \cos 2\alpha\,, \qquad (11)$$

$$k_{\rm sp} = K_{\rm sp}/\tan(2\alpha)\,. \qquad (12)$$

Consequently, the tilting angle δ depends on $K_{\rm s}$, $K_{\rm sp}$ and $K_{\rm dip}$ but does *not* depend on $K_{\rm u}$. It would also depend on $K_{\rm b}$ if the bulk anisotropy was accounted for but such dependence is very weak since $K_{\rm b} \ll K_{\rm s}$, $K_{\rm sp}$ as explained above.

The choice between θ'_0 and $\theta'_0 + 90°$ which both satisfy Eq. (10), is done based on the energy minimum auxiliary condition $\partial^2 E_\perp(\theta')/\partial\theta'^2 > 0$, where the second-order derivative is given by $2(K_{\rm s} - \widetilde{K}_{\rm dip})/\cos 2\theta'_0$ or, equivalently, $2\tan 2\alpha(k_{\rm sp} - \widetilde{K}_{\rm dip})/\sin 2\theta'_0$. Thus we obtain two values of the tilting angle θ'_0 and $\theta'_0 + 180°$ corresponding to the opposite directions of magnetization for which the film energy is the same in the absence of external fields. These two directions are equivalent and define the same easy axis of magnetization. The model does not distinguish between them, and one of the directions needs to be chosen arbitrarily as the magnetization direction. Naturally, these directions are distinguishable in MOKE experiment and are determined by the applied magnetic field direction, as shown schematically in Fig. 1(b). In this work, we will consistently consider the magnetization vector with a longitudinal component pointing towards $[33\bar{1}]$ crystallographic direction, i.e., towards the right side of the sample in the α^+ configuration, as shown in Fig. 1(a) and (b). In the absence of external fields, for the sample in *a virgin* magnetic state, stripe domains with alternating magnetization orientations θ'_0 and $\theta'_0 + 180°$ are formed, as it was shown by SPLEEM experiment[16].

C. Relations between anisotropy constants and tilting angle: superposition of uniaxial anisotropies. Effective uniaxial anisotropy

The analytical formula (10) for θ'_0 provides also more qualitative predictions of how the tilting angle depends on the three scaled anisotropy constants $\widetilde{K}_{\rm dip}$, $K_{\rm s}$, $k_{\rm sp}$. There are six possible different cases of mutual relations between these constants, like $K_{\rm s} < k_{\rm sp} < \widetilde{K}_{\rm dip}$, which correspond to six distinct (non-overlapping) intervals of δ which cover the full range of the tilting angle. There are also six borderline cases where two of the anisotropy constants are equal which leads to a specific value of δ in each case.

All these cases are presented in Fig. 3, which clearly shows how the tilting angle δ evolves when the values of $\widetilde{K}_{\rm dip}$, $K_{\rm s}$, $k_{\rm sp}$ change, e.g., due to increasing thickness of the Fe film $N_{\rm Fe}$ or due to covering the film with the Au overlayer. The figure can also be used in a reverse way to predict how the anisotropy constants evolve, e.g., with increasing $N_{\rm Fe}$, to reproduce the dependencies of the tilting angle δ on the Fe and Au layer thicknesses observed experimentally. The reverse predictions are largely semi-quantitative since one cannot determine exactly two unknown variables: $K_{\rm s}$ and $k_{\rm sp}$ on the basis of one known quantity, i.e., δ. However, the two MCA constants and $\widetilde{K}_{\rm dip}$ must satisfy the inequality relations which uniquely correspond to each value of the experimental tilting angle, according to the scheme shown in Fig. 3. In addition, if specific values of the tilting angle, like $\delta = \pm45° + \alpha$ and $\delta = \alpha$ or $\delta = -90° + \alpha$ (or equivalent tilting angles) are observed for Fe or Au/Fe films at specific thicknesses of Fe film or Au overlayer, the equality relations $K_{\rm s} = \widetilde{K}_{\rm dip}$ and $k_{\rm sp} = \widetilde{K}_{\rm dip}$, respectively, must hold. Then, the corresponding anisotropy constants are determined exactly for the films of the specific thickness since the values of $\widetilde{K}_{\rm dip}$ are known. Also, another strict condition $K_{\rm s} = k_{\rm sp}$ is imposed on the anisotropy constants of the particular films for which one of the following tilting angles, $\delta = 0°$, $\delta = \pm90°$ or $\delta = 180°$, is found.

The obtained relation between the anisotropy constants $K_{\rm dip}$, $K_{\rm s}$ and $K_{\rm sp}$ and the tilting angle δ can be explained by superposition of three uniaxial anisotropies within the plane perpendicular to the steps; see Figs. 3 (b) and (c). Each of them is described by an energy dependence $K\sin^2(\theta - \theta_{\rm ea})$, where K denotes the corresponding anisotropy constant and the polar angle $\theta_{\rm ea}$ determines orientation of the respective easy magnetization axis. This orientation is given by $\theta_{\rm ea} = 90°$ for the shape anisotropy and $\theta_{\rm ea} = -\alpha$ (or equivalently $180° - \alpha$) for the perpendicular MCA term with $K_{\rm s} > 0$. For $K_{\rm sp} > 0$ the corresponding easy axis is determined by $\theta_{\rm ea} = 45° - \alpha$.

Superposition of two uniaxial anisotropies, described by the sum of their energies, is also a uniaxial anisotropy and the resultant easy axis is oriented in the acute angle between the two easy axes of the contributing anisotropies[37]. For superposition of the perpendicular ($K_{\rm s}$) and the step-induced ($K_{\rm sp}$) magnetocrystalline anisotropies we find that the effective easy axis is rotated from the easy axis of the perpendicular magnetocrystalline anisotropy towards the easy axis of the step-induced anisotropy. The rotation angle $\Delta\theta_0^{\rm s,sp}$ is less than α if $k_{\rm sp} < K_{\rm s}$, while otherwise this angle is larger than α. In the former case the effective easy axis of the two anisotropies is oriented at the polar angle $180° - \alpha < \theta_{\rm ea}^{\rm s,sp} < 180°$, while for $k_{\rm sp} > K_{\rm s}$ the orientation of the effective easy axis is described by $180° < \theta_{\rm ea}^{\rm s,sp} < 225° - \alpha$ or equivalently by $0° < \theta_{\rm ea}^{\rm s,sp} < 45° - \alpha$.

Therefore, when the effective magnetocrystalline uniaxial anisotropy is added to the shape anisotropy it re-
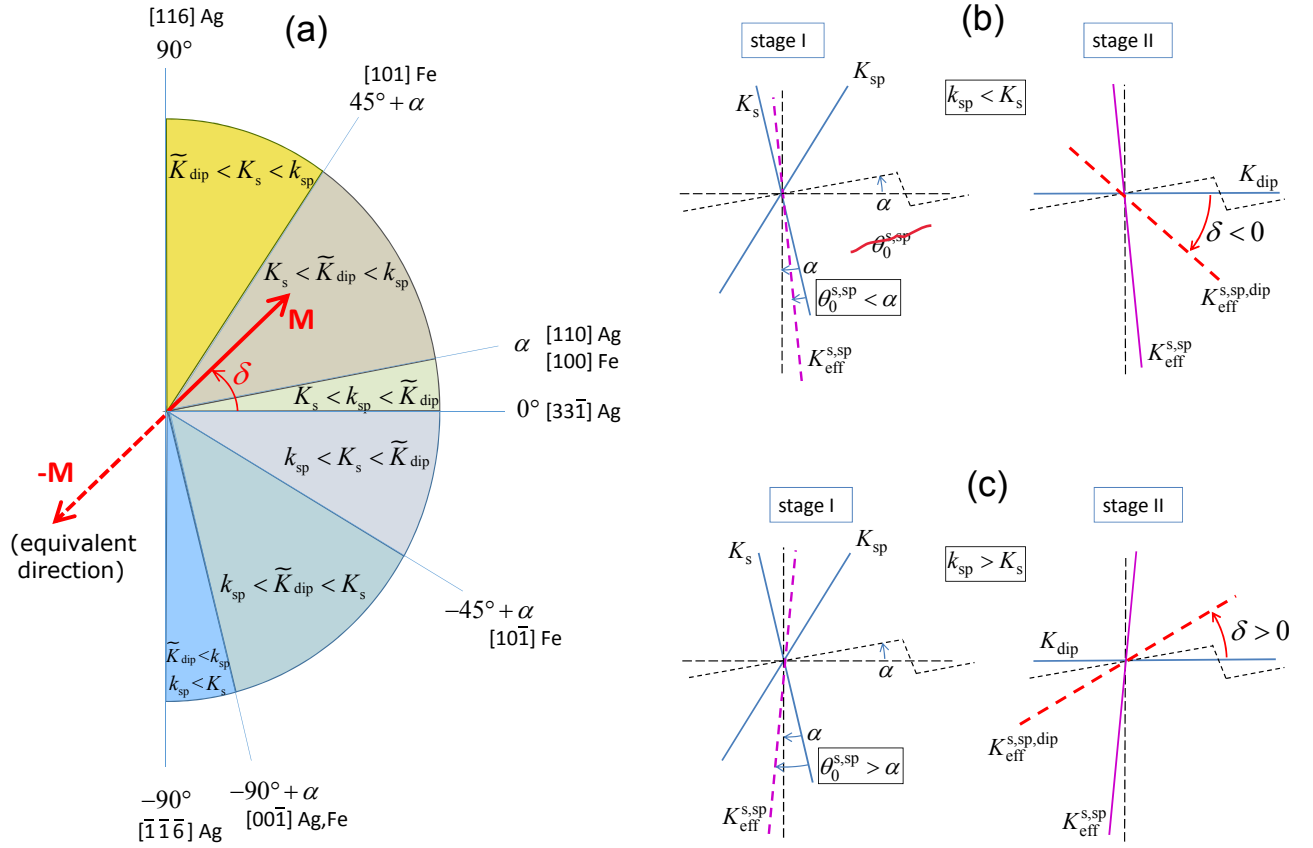
FIG. 3: (a) Tilting angle versus magnetic anisotropy constants. (b,c) Superposition of three uniaxial anisotropies within the plane perpendicular to the steps, carried out in two stages. The effective anisotropy $K_{\mathrm{eff}}^{\mathrm{s,sp}}$ is obtained by superposing the magnetocrystalline anisotropies K_{s} and K_{sp} in stage I and subsequently added to the shape anisotropy K_{dip} in stage II, resulting in the final effective uniaxial anisotropy $K_{\mathrm{eff}}^{\mathrm{s,sp,dip}} = K_{\mathrm{eff},\perp}$. The superposition is done in the two cases: (b) $k_{\mathrm{sp}} < K_{\mathrm{s}}$ and (c) $k_{\mathrm{sp}} > K_{\mathrm{s}}$.

sults in the final effective uniaxial anisotropy with the easy axis oriented either at negative or positive tilting angle δ depending on whether k_{sp} is smaller or larger than K_{s}, respectively; see Fig. 3 (b), (c). While orientation of the easy axis of the effective anisotropy is given by Eq. (10), the magnitude of the corresponding anisotropy energy $E_{\perp}(\theta) = E_{\perp}(\theta_0) + K_{\mathrm{eff},\perp} \sin^2(\theta - \theta_0)$ is given by the effective anisotropy constant expressed as follows:

$$K_{\mathrm{eff},\perp} = \sqrt{(\widetilde{K}_{\mathrm{dip}} - K_{\mathrm{s}})^2 + \tan^2 2\alpha \, (\widetilde{K}_{\mathrm{dip}} - k_{\mathrm{sp}})^2} \, . \quad (13)$$

The above considerations are strictly correct for the films where the spontaneous magnetization is oriented within the vertical plane perpendicular to the steps. If the easy axis is parallel to the steps, an external magnetic field is necessary to align magnetization perpendicular to the steps. If the field is applied in-plane perpendicular to the steps, it needs to be equal to or larger than the shift field H_{s}, since that is the field value required to switch the magnetization to the direction within vertical plane perpendicular to the steps. In the case of Fe/Ag(116), the easy magnetization axis switches to the direction parallel to the steps only when the absolute value $|\delta|$ of the tilting

angle becomes small (as shown in[16] and Sec. IV) and the applied external field has negligible effect on the tilting angle value.

D. Role of k_{sp}

According to Fig. 3, the sign of the tilting angle δ depends on the value of k_{sp} with respect to K_{s}. For positive K_{s} (as expected for Fe films), the angle δ is positive if $k_{\mathrm{sp}} > K_{\mathrm{s}}$, while negative if $k_{\mathrm{sp}} < K_{\mathrm{s}}$. The inclusion of the anisotropy constant k_{sp} in the theoretical model can thus be crucial for a proper reproduction of the tilting angle observed experimentally.

In particular, the magnetization of a stepped film cannot orient perpendicular to the steps and parallel or perpendicular to the film surface, i.e., along the $\delta = 0°$ or $\delta = 90°$ directions, respectively, if k_{sp} is neglected. Also, for $k_{\mathrm{sp}} = 0$, magnetization cannot be oriented perpendicular to the terrace plane ($\delta = 90° + \alpha, -90° + \alpha$). In addition, the *positive* tilting angle within the interval $0 < \delta \leq 90° + \alpha$ (or the equivalent interval $-180° < \delta \leq$

$-90º + \alpha$) is *not* allowed for $k_{\rm sp} = 0$ and positive $K_{\rm s}$. Indeed, if $k_{\rm sp} = 0$ and $K_{\rm s} > 0$, the possible relations betweeen the three anisotropy constants $k_{\rm sp}$, $K_{\rm s}$ and $K_{\rm dip}$ correspond to the tilting angle $-90° + \alpha < \delta < 0$ or equivalently the tilting angle $90° + \alpha < \delta < 180°$. The fact that orientations of the easy axis which are not allowed for $k_{\rm sp} = 0$, like those with a positive tilting angle, are observed experimentally, means that the anisotropy energy indeed must include the finite step-induced term $k_{\rm sp}$.

IV. EXPERIMENTAL VERIFICATION OF THE MODEL

A. Experimental MOKE results - tilting angle

The theoretical model presented here shows that magnetization of a Fe film can be tilted due to broken symmetry of the vicinal surface. The tilting angle can be either positive or negative, depending on three anisotropy constants $K_{\rm dip}$, $K_{\rm s}$ and $k_{\rm sp}$. In order to evaluate the tilting angle experimentally and compare it with the theoretical model, MOKE measurements are performed in two different longitudinal geometries: α^+ (perpendicular to the steps) and α^- (perpendicular to the steps after 180° rotation of the sample). Representative hysteresis loops measured in the geometry α^- at 5 K are shown in Fig. 4 and they are counterparts of the loops shown in Fig. 1 measured in the geometry α^+.

Depending on the thickness of the Fe film, the easy magnetization axis can be oriented parallel or perpendicular to the steps. Thus, by applying the magnetic field perpendicular to the steps, split loops or square loops are observed, respectively (Figs. 1 and 4). The Kerr ellipticity extracted from both square and split hysteresis loops can be unambiguously defined as the Kerr ellipticity ϕ^H at H_s, i.e., at the minimum field necessary to switch the magnetization to the direction perpendicular to the steps. Therefore, in the case of the easy magnetization axis oriented along the steps, the Kerr signals $\phi^H_{\alpha-}$ and $\phi^H_{\alpha+}$ measured perpendicular to the steps require a finite magnetic field and correspond to the orientations of the intermediate axis rather than the easy axis. Naturally, in the case of the easy magnetization axis oriented perpendicular to the steps, square loops are measured and therefore $\phi^H_{\alpha-}$ and $\phi^H_{\alpha+}$ correspond to the Kerr ellipticities at remanence (i.e., $H_s = 0$). The choice of $\vec{H}$ at which ϕ^H is evaluated from the hysteresis loops measured perpendicular to the steps is important because ϕ^H depends on $\vec{H}$ due to the tilting angle of magnetization. After applying sufficiently large magnetic field $\phi^H_{\alpha-}$ and $\phi^H_{\alpha+}$ will correspond to the saturation values, hence to the Kerr ellipticity of the magnetization oriented in the sample plane. As seen in Fig. 1(c) and 4(c) the Kerr signal depends very weakly on the field H of moderate magnitude larger than H_s, and therefore the longitudinal

and polar Kerr signals are still well defined once the field switches the magnetization to the direction perpendicular to the steps.

The Kerr ellipticity measured at α^+ and α^- geometries consists of longitudinal and polar contributions arising from the respective components of the magnetization. The idea of separation of longitudinal and polar components is schematically illustrated in Figs. 1(b) and 4(b) for negative tilting angle, $\delta < 0$. In this case, when the magnetization is probed in the α^+ geometry, at positive $\vec{H}$ the polar component ϕ_P of the Kerr signal is negative and adds to the positive longitudinal component ϕ_L, while at negative $\vec{H}$ the magnetization is reversed and the positive polar component ϕ_P adds to the negative longitudinal component ϕ_L. On the contrary, when the magnetization is probed in the α^- geometry, at positive $\vec{H}$ the positive ϕ_P adds to the positive ϕ_L and after reversing the $\vec{H}$, the negative ϕ_P adds to the negative ϕ_L. One can therefore notice that the longitudinal signal ϕ_L has always the same sign as the applied magnetic field, regardless of the geometry, but the sign of the polar Kerr signal ϕ_P depends on the sign of the tilting angle and is always reversed while changing between these two geometries.

In the case of the hysteresis loops measured for uncovered Fe films the polar Kerr signal is additive in the α^- geometry [Fig. 4(c),(e)] and subtractive in the α^+ geometry [Fig. 1(c),(e)]. As a result, the hysteresis loops measured at α^+ are reversed, i.e., show positive signal at negative magnetic field and negative signal at positive magnetic field). With decreasing the Fe thickness, in particular below 6 ML of Fe, the coercivity increases. This is associated with the SRT from in-plane to out-of-plane orientation of magnetization. Therefore, the magnetic field which is applied in the sample plane, has to be larger in the vicinity of SRT, since the out-of-plane component of the magnetization becomes dominant. For thicknesses lower than 4 ML, magnetization could not be switched even with the maximum available magnetic field 6000 Oe. Note however that by using MOKE in the polar geometry (i.e. by applying magnetic field perpendicular to the sample plane), square hysteresis loops are detectable down to 2 ML of Fe.

In order to obtain more quantitative information about the magnetization from the hysteresis loops measured perpendicular to the steps, a deconvolution of the total Kerr signal into the longitudinal ϕ_L and polar ϕ_P components has to be performed. By measuring $\phi^H_{\alpha+}$ and $\phi^H_{\alpha-}$, the longitudinal ϕ_L and polar ϕ_P Kerr ellipticities can be obtained from[17]:

$$\phi_L = \left(\phi^H_{\alpha+} + \phi^H_{\alpha-}\right)/2 \qquad (14)$$

$$\phi_P = \left(\phi^H_{\alpha+} - \phi^H_{\alpha-}\right)/2 \qquad (15)$$

Since the mixture of ϕ_L and ϕ_P components is a consequence of tilted magnetization (δ), one can use these
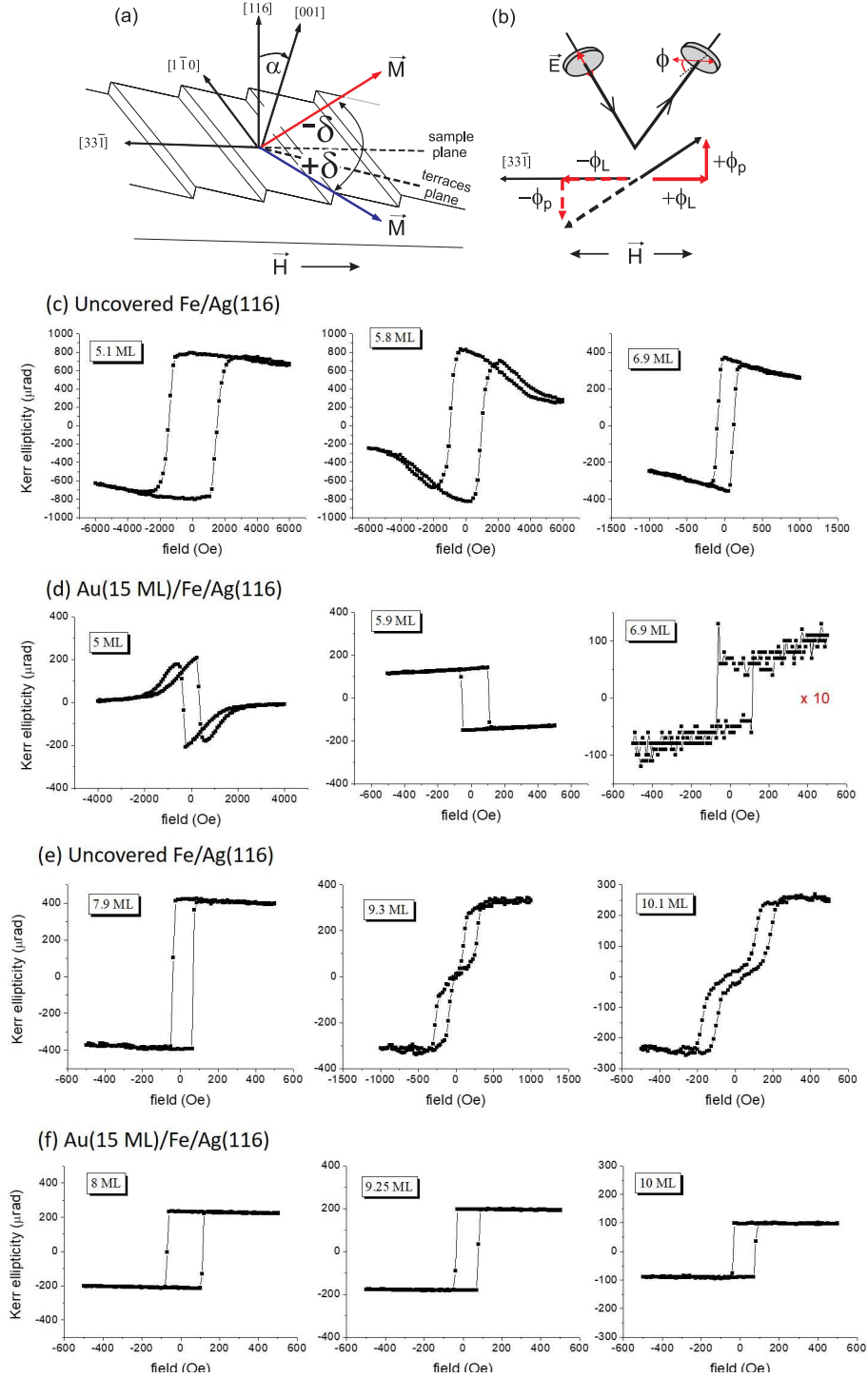
FIG. 4: (a) Crystallographic directions and corresponding possible canted magnetization orientations within the plane perpendicular to the steps for FM film on the (116) vicinal surface in the geometry α^-, i.e., after rotation of the sample by 180° with respect to Fig. 1(a). Magnetization vectors with positive and negative tilting angles are shown by blue and red arrow, respectively. (b) Schematics of LMOKE measurement and LMOKE signal decomposition into longitudinal (ϕ_L) and polar (ϕ_P) components (again, only the case of negative tilting angle is shown). Hysteresis loops measured at α^- geometry at $T = 5$ K for uncovered (c),(e) and covered with Au (d),(f) Fe films with different thicknesses.
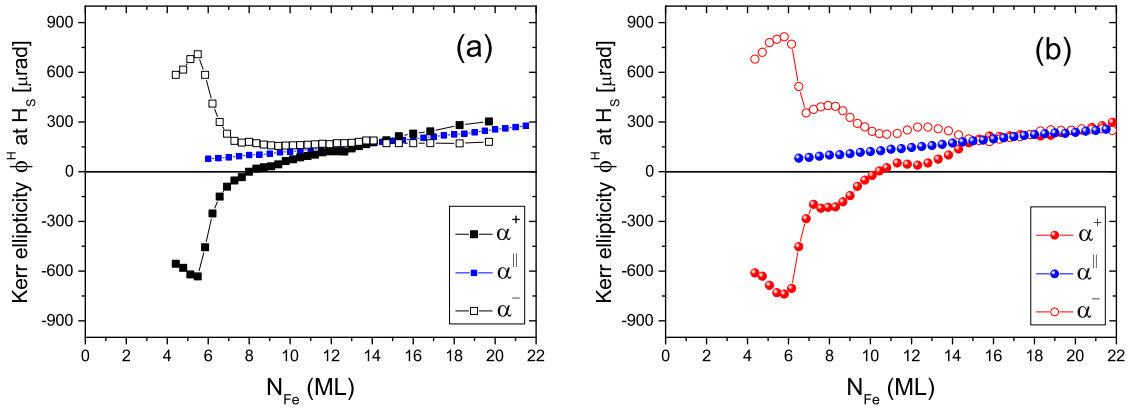
FIG. 5: Kerr ellipticity ϕ^H at H_s as a function of thickness of Fe film grown on Ag(116) surface obtained from hysteresis loops measured at (a) T = 300 K and (b) T = 5 K

values to estimate δ quantitatively. Indeed, the tilting angle δ can be extracted from:

$$\tan \delta = \frac{M_z}{M_y} = \frac{\phi_P}{\phi_L} \frac{\phi_L^s}{\phi_P^s} \qquad (16)$$

where ϕ_L^s and ϕ_P^s are the saturation Kerr signals in longitudinal and polar geometries, respectively. The saturation longitudinal Kerr signal ϕ_L^s can be obtained from the Kerr signal measured in $\alpha^{\|}$ geometry (in which the magnetic field is applied along the steps), however, only in the case of δ smaller than $\sim 10°$. For larger δ, the available magnetic field is usually not sufficient to saturate magnetization along the steps ($\alpha^{\|}$). Fortunately, since the theory of MOKE in ultrathin FM films has been well developed[17,27,28,38], the ratio of the longitudinal and polar saturation signals can be calculated theoretically by utilizing the values of the refractive indices[39,40] and the Voight constant of $\mathcal{Q}_{Fe} = 0.376 + 0.0066i$[41]. Since the polar Kerr effect is much stronger than the longitudinal one, even tiny changes of the tilting angle δ (of the order of $\sim 1°$) are detectable by longitudinal MOKE with the in-plane magnetic field applied perpendicular to the steps[17].

The dependence of Kerr ellipticity ϕ^H at H_s on Fe thickness for three geometries α^+, α^- and $\alpha^{\|}$ is shown in Fig. 5. It is immediately visible that Kerr ellipticity ϕ^H measured at α^+ and α^- geometries is significantly different than measured at $\alpha^{\|}$, indicating changes of polar Kerr contribution ϕ_P related to normal component of the magnetization. Note however that the increase of ϕ^H at H_s does not automatically means the increase of the tilting angle value, as both polar and longitudinal Kerr signals change with thickness. Negative values of ϕ^H denote that measured hysteresis loops were reversed. At 5 K, oscillatory behavior of ϕ^H is observed when probed at α^+ and α^-. The fact that oscillatory behavior of ϕ^H is observed only at low temperature and only at α^+ and α^- geometries (no oscillations at $\alpha^{\|}$), clearly indicates that

the oscillations of ϕ^H observed in our experiment are not related to the oscillatory magneto-optical effects (keeping in mind that oscillatory magneto-optical Kerr effect can be observed when QWS from unoccupied sp-states are formed)[42,43]. Instead, the oscillations of ϕ^H result from the oscillatory changes of the polar component of magnetization.

The longitudinal ϕ_L and polar ϕ_P contributions to the total Kerr ellipticity were calculated according to the equations (14) and (15). Consequently, the tilting angle δ of magnetization was obtained from the formula (16). The dependence of δ on Fe film thickness of uncovered sample at 300 K is shown in Fig. 6(b). For uncovered Fe films thicker than 15 ML, the tilting angle δ is positive, slightly exceeding zero. It means that the magnetization is tilted from the sample plane towards the terraces plane (with δ defined as shown in Fig. 1(a)). With decreasing thickness of the Fe film, δ decreases changing its sign at around 13 ML and becomes negative. Below 8 ML, tilting angle changes rapidly due to SRT and reaches the maximum value $\delta = -76°$ for ~ 5 ML. This angle corresponds roughly to [001] direction, which for bare Ag(116) crystal is oriented 13.3° off the sample normal, i.e., is equivalent to $\delta = -76.7°$.

At 5 K the overall changes of δ are similar as at 300 K, but additional, oscillatory behavior of δ as a function of Fe thickness is observed (Fig. 6(d)). Three extrema of δ can be distinguished at ~ 8.5 ML, ~ 12.8 ML and ~ 18.7 ML, which are the same thicknesses of Fe (within the experimental error ± 0.3 ML), at which maxima of the photoemission spectroscopy and the anisotropy of the orbital magnetic moment were observed[21]. Therefore, the oscillatory changes of δ with increasing Fe film thickness are due to the quantization of d states with Δ_5 spatial symmetry[21]. The oscillations of δ are perturbed below ~ 7 ML of Fe due to a rapid change of the tilting angle related to SRT. As already mentioned, below 4 ML of Fe, the hysteresis loops could not be measured due to large coercivity exceeding the maximum available mag-

netic field.

Covering the Fe films with a 15 ML-thick overlayer of Au changes the dependence of the tilting angle dramatically. In particular, at $T = 300$K the tilting angle of the magnetization becomes positive (Fig. 7(b)). It is close to $\delta = +70°$ for the film thickness of 2.5 ML and quickly decays with increasing Fe thickness reaching a nearly in-plane direction, $\delta = 0°$, for $N_{Fe} \geq 5$ ML. At low temperature of $T = 5$ K, tilting angle oscillates with increasing thickness of the Fe film and the oscillations are more pronounced than for the uncovered films at the same temperature (Fig. 7(d)). The oscillatory dependence leads to negative tilting angle, reaching almost $\delta = -20°$, in the thickness range from 7 to 10 ML. For thicker films, the tilting angle oscillates around $\delta = 0°$, but the oscillation amplitude does not exceed a few degrees. The extrema of δ can be distinguished at ~ 8.4 ML and ~ 13 ML, i.e., at the same thicknesses of Fe (within the experimental error ± 0.3 ML) as for the uncovered sample.

B. Fitting anisotropy constants to tilting angle of experimental magnetization of Fe/Ag(116) and Au/Fe/Ag(116) films

To reproduce the experimental tilting angle δ in the described model one needs to fit two magnetocrystalline anisotropy constants: K_s and K_{sp} (or k_{sp}) since the shape anisotropy constant K_{dip} is known. The third magnetocrystalline constant K_u does not need to be accounted for since it does not affect the tilting angle (though it affects the shift field, which is not discussed in this article).

The model provides exact values of K_s and k_{sp} for the Fe film thicknesses at which δ attains some specific values. In particular, the following relations must be satisfied for Fe/Ag(116) films: $K_s = \widetilde{K}_{dip}$ if $\delta = -45° + \alpha = -31.7°$ and $k_{sp} = \widetilde{K}_{dip}$ if $\delta = -90° + \alpha = -76.7°$. The model also predicts $k_{sp} = K_s$ at the Fe thickness for which $\delta = 0°$. These are the basic bounds imposed on the fit of the anisotropy constants in our model for the Fe/Ag(116) films. While applying the above relations we assume $K_{dip} = 0.142 \times N_{Fe}$ meV/(surface atom) corresponding to the saturation magnetization of $M = 1725$ emu/cm^3 in bulk Fe. bulk.

For uncovered Fe films thicker than 10 ML we take $K_s = 1.77$ erg/cm$^2 = 0.91$ meV/(surface atom) obtained as the sum of the experimental values of K_s(Fe/Ag) $= 0.81$ erg/cm^2 and K_s(Fe/vacuum) $= 0.96$ erg/cm^2 found by Heinrich et al. for the Fe/Ag(001) flat films.[44] To meet the condition $K_s = \widetilde{K}_{dip}$ for the film thickness $N_{Fe} = 6.2$ ML at which the tilting angle is $\delta = -31.7°$ at $T = 300$ K, the anisotropy constant K_s is assumed to decrease with decreasing the Fe thickness below 10 ML. The decrease is described with a quadratic function in a good agreement with the experimental trends. In particular, a rapid decrease of K_s for the Fe thickness less than 7 ML – with K_s at 3 ML dropping to around half of K_s at 7 ML – was observed for flat Fe/Ag(001) films in the Brillouin light

scattering (BLS) experiment by Hicken et al.[36]. Also our previous fits based on the SPLEEM measurements[16] predict a monotonic decrease of K_s and k_{sp} in the whole investigated thickness range from 5.6 to 2.8 ML of Fe.

Such decrease of K_s can be attributed to the presence of Ag atoms on the upper surface of the Fe films so that the anisotropy constant K_s for the nominally uncovered Fe film becomes closer to K_s for the Fe film covered with Ag. Such an explanation is supported by the finding of Hicken et al[36] who reported that covering Fe(3.2 ML)/Ag(001) with an Ag overlayer changes K_s by 0.025 erg/cm^2 only (from 0.43 to 0.405 erg/cm^2) which is much smaller than the change of K_s by 0.15 erg/cm^2 (from 0.66 to 0.51 erg/cm^2) upon covering Fe(6 ML)/Ag(001) with Ag. The segregation of Ag atoms on top of Fe/Ag(001) films have been reported for the growth of Fe(10 ML) at elevated temperatures (500 K) and for the growth of Fe films with the thicknesses from 4 to 6 ML at 150 K followed by annealing at 500-550 K.[45,46]

We also assume that the two anisotropy constants k_{sp} and K_u, which come into play when a Fe film is deposited on the stepped Ag substrate, have bulk-like contributions proportional to the Fe thickness. The contributions result from the film structure, more precisely from its local symmetry, which is severely disturbed in each Fe atomic layer by stacking faults which develop throughout the Fe film thickness over each step on the Ag(116) surface. Such defects arise due to the large vertical mismatch of around 42% between the interlayer distances in fcc-Ag and bcc-Fe. The linear dependence of k_{sp} on the Fe thickness N_{Fe} is assumed for $N_{Fe} > 10$ML and also includes a constant term corresponding to the interfaces of the Fe film. For thinner Fe films we allow for deviations from the linear dependence and describe the anisotropy constant by a quadratic function of N_{Fe} in a similar way as we do for K_s. All fitted dependencies of the anisotropy constants on the Fe thickness are assumed to be continuous and to have a continuous slope. In this way our theoretical model reproduces accurately the tilting angle observed experimentally for uncovered Fe films grown on the Ag(116) substrate using the simple dependencies of the fitted anisotropy constants K_s and k_{sp} on the Fe thickness shown in Fig. 6. Note that the plotted quantities k_{sp} and $\widetilde{K}_{dip}$ are scaled anisotropy constants. The original step-induced anisotropy constant $K_{sp} = k_{sp} \tan 2\alpha$ is smaller than k_{sp} by the factor of 0.501 for Fe films on the (116) Ag substrate while the shape anisotropy constant K_{dip} is $\widetilde{K}_{dip}/\cos 2\alpha = 1.12\widetilde{K}_{dip}$.

For Fe/Ag(116) films covered with 15 ML-thick layer of Au, the model readily provides the values of k_{sp} and K_s equal to $\widetilde{K}_{dip}$ for the thicknesses of Fe for which the experimental tilting angle is $\delta = \alpha = 13.3°$ and $\delta = 45° + \alpha = 58.3°$, respectively. At $T = 300$ K, the constant k_{sp} has to be larger than K_s to keep the tilting angle positive for all Fe thicknesses as is found experimentally, whereas the almost vanishing tilting angle ($\delta = 0°$) for the Fe thickness range of 5-7 ML requires k_{sp} almost equal to K_s.
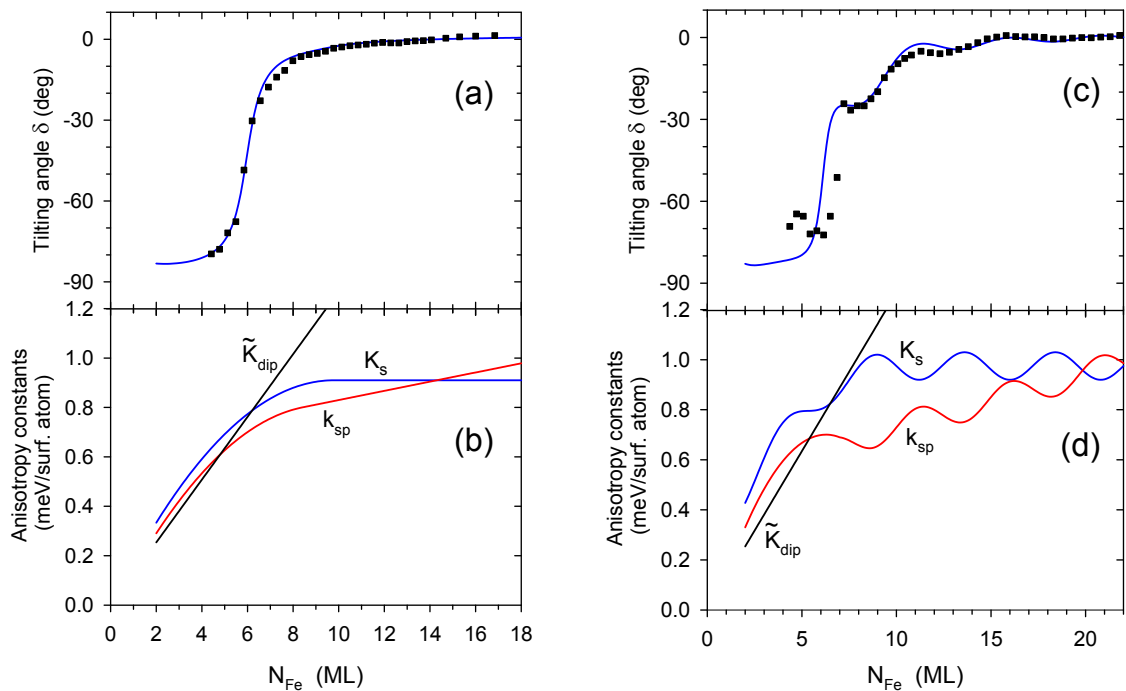
FIG. 6: (a,c) Experimental values of tilting angle δ (squares) as a function of the thickness of Fe films on Ag(116) and the theoretical dependence δ vs N_{Fe} (solid line) obtained by fitting (b,d) the model dependences of the anisotropy constants; (a,b) T = 300 K and (c,d) T = 5 K.
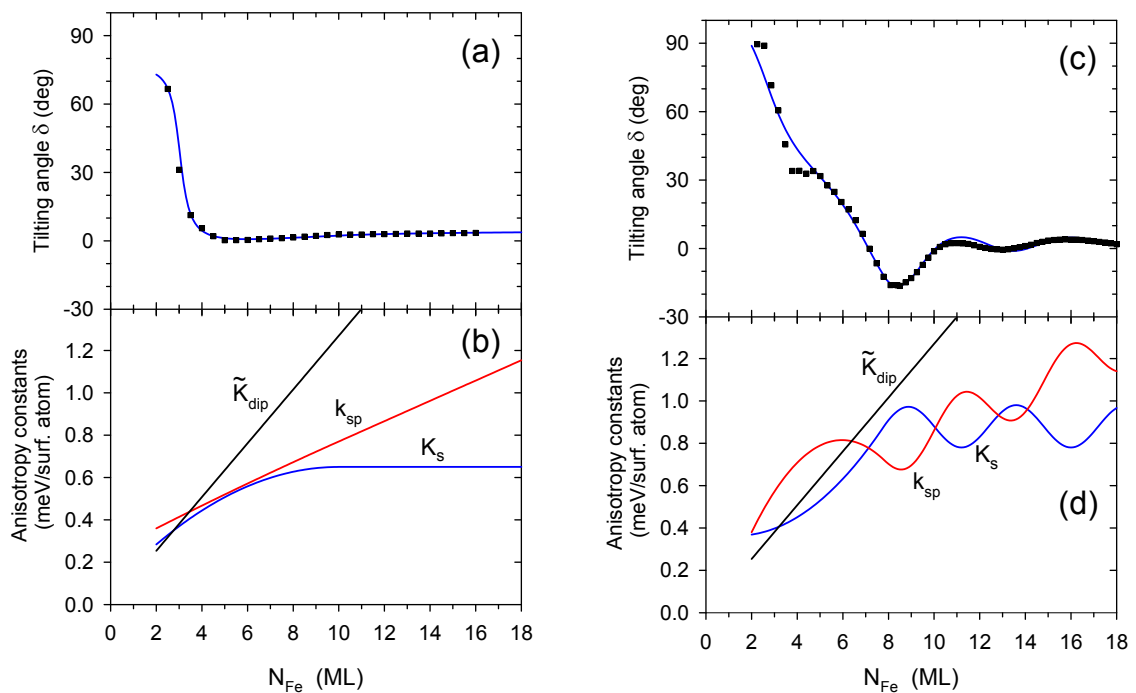

FIG. 7: (a,c) Experimental values of tilting angle δ (squares) as a function of the thickness of Au(15 ML)-covered Fe films on Ag(116) and the theoretical dependence δ vs N_{Fe} (solid line) obtained by fitting (b,d) the model dependences of the anisotropy constants; (a,b) T = 300 K and (c,d) T = 5 K.
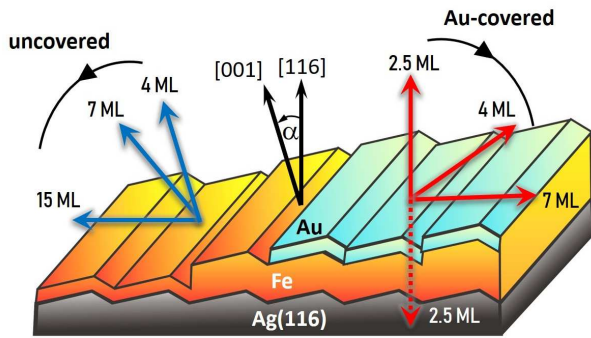
FIG. 8: Schematic of the magnetization direction changes for uncovered and Au-covered Fe films upon increasing the Fe film thickness (left and right side of the sample, respectively), as obtained from MOKE measurements of the tilting angle at 5 K. Note that all magnetization orientations represent the easy axes directions and therefore possess $+180°$ equivalent orientations, as indicated for 2.5 ML of Au-covered sample.

The step-induced anisotropy constant k_{sp} of the Au-covered Fe films is also assumed to grow linearly with the thickness of Fe for $N_{Fe} > 10$ ML due to the stacking faults. The slope of the k_{sp} linear dependence on thickness is larger than the corresponding slope for Fe/Ag(116), which can be attributed to different relaxation of the atomic structure in the interior of the Fe film if the Au cap is present. The value of K_s is assumed to be constant for $N_{Fe} > 10$ ML but shifted downwards in comparison with Fe/Ag(116) to 0.65 meV/(surface atom), which is the value measured for Au/Fe/Ag(001) by Heinrich et al.[44]. For the Fe films thinner than 10 ML, the best fits of K_s and k_{sp} are obtained by using quadratic functions, similarly as in the case of uncovered films. The theoretical model based on the so obtained dependencies of K_s and k_{sp} on Fe thickness provides an excellent fit to the experimental tilting angle for the Au-covered Fe films at $T = 300$ K.

The fits of anisotropy constants measured at $T = 300$ K are the starting point for the $T = 5$ K fits. The oscillatory contributions of sinusoidal form are first added to the room-temperature fits of K_s and k_{sp} for $N_{Fe} > 7$ ML followed by small constant shifts to improve the fits. The extra shifts can be attributed to the temperature dependence of the anisotropy (or rather its part not related to the quantum well states). With a suitably chosen phase of the K_s oscillations we successfully reproduce the shallow minimum of the magnetization tilting angle for the uncovered Fe films at around 8 ML of Fe.

Since the oscillations originate from QWS regularly crossing the Fermi level with increasing the Fe thickness[47,48], all magnetocrystalline anisotropy constants (K_s, k_{sp}, and also K_u) have either the same phase or some of them oscillate in antiphase with respect to

the others. The reason for this is that originally each anisotropy constant is defined as a difference of two energies, corresponding to two relevant magnetization directions [Eq. (4)]. While the second-order perturbation theory predicts that a quantized state (coupled to electronic states of opposite occupancy by the spin-orbit interaction) gives a negative contribution to the film energy, this contribution varies with magnetization direction due to the change of the spin-orbit matrix elements and can even vanish for some directions due to symmetry. Therefore, the contribution of such a state to each of the two concerned energies can be different and as a result its contribution to the anisotropy constant defined as the difference of these energies can be either positive or negative. This possibility is exploited in the present fit by assuming that the anisotropy constants K_s and k_{sp} oscillate in antiphase with increasing the Fe thickness.

The obtained fits accurately reproduce the experimental tilting angle for both Fe/Ag(116) and Au/Fe/Ag(116) films at 5 K. The fitted oscillation period of the anisotropy constants in both samples is 4.8 ML. Note that the period of the magnetic anisotropy oscillations observed in experiment is not constant and changes with the Fe film thickness, from ~ 5.7 ML[19] in the thick Fe limit, down to ~ 4.1 ML for thicknesses below 10 ML[21]. Such thickness dependent oscillation period can be ascribed to the lattice relaxation of the Fe film[49], which in consequence can modify the electronic structure, and therefore also Δ_5 band forming QWS. The extrema of δ at ~ 8.5 ML, ~ 12.8 ML and ~ 18.7 ML obtained in the present MOKE measurements appear at the same Fe thicknesses at which QWS and the anisotropy of the orbital moment were previously observed[16]. It corresponds to the period of ~ 4.3 ML and ~ 5.9 ML, respectively, which on average gives ~ 5.1 ML and hence agrees (within the experimental error ± 0.3 ML) with the theoretical value of 4.8 ML.

For the Au/Fe/Ag(116) films, at $T = 5$ K, the fitted oscillations of the anisotropy constants have the same phase as for the Fe/Ag(116) films and both K_s and k_{sp} are shifted upwards with respect to their RT values (and their shifts are larger in comparison to uncovered Fe films). The dependencies of K_s and k_{sp} on thickness satisfy the conditions $K_s = \tilde{K}_{dip}$ and $k_{sp} = \tilde{K}_{dip}$ at the Fe thicknesses of 3.2 ML and 7.15 ML for which the specific values of $\delta = 45° + \alpha = 58.3°$ and $\delta = +\alpha = 13.3°$ are observed, respectively.

Based on the MOKE experimental results and the fits to the model we find that the orientation of the easy axis at $T = 5$ K approaches the direction perpendicular to the terraces plane in the case of uncovered sample and perpendicular to the sample plane in the case of Au-covered sample (i.e., along [001] and [116] crystallographic directions, respectively). Although there are no experimental data points for uncovered films below 4 ML of Fe, previous SPLEEM results including thinner Fe films show that the tilting angle does not change substantially within this thickness range[16]. Upon increase of the Fe film thick-

ness, the magnetization rotates continuously following the changes of the tilting angle shown in Figs. 6 and 7. The direction of the rotation is different for the two considered types of systems: it is anticlockwise for the Fe/Ag(116) films and clockwise for the Au/Fe/Ag(116) films viewed in the $\alpha+$ configuration [Fig. 1(a)] as illustrated schematically in Fig. 8. Obviously, this rotation direction is reversed if it is viewed in the $\alpha-$ configuration [Fig. 4(a)]. For the thinnest measured Fe thicknesses of uncovered and Au-covered films the magnetization directions (i.e., the easy axes) are originally aligned along [001] and [116] crystallographic directions, respectively, and therefore divergent only by $\sim 13.3°$. Upon increasing the Fe thickness the directions of magnetization easy axes in the two types of films become very different and at 4 ML are nearly orthogonal (Fig. 8). With further increase of the Fe thickness, the two easy axes become again close to each other as they approach in-plane direction, perpendicular to the steps.

The herein reported results of the MOKE experiments for uncovered Fe films are consistent with previous measurements of domain structure with SPLEEM[16]. Although the orientations of the canted magnetization in SPLEEM experiments have been acquired in the absence of magnetic field and at different temperature T = 130 K (Fig. 2 of Ref.[16]), they agree very well with the presently obtained values of the tilting angle for uncovered sample at T = 300 K (Fig. 6(b)). The comparison of the results of the two different experiments confirms the validity of our method for probing the canted state of magnetization by using MOKE in longitudinal geometry.

V. EFFECT OF VARYING Au COVERAGE ON MAGNETIZATION DIRECTION

In order to get more insight into the effect of Au on magnetic anisotropy of the underlying FM film, MOKE measurements were performed on 13 ML thick Fe film covered by Au wedge. Covering with Au remarkably affects the Kerr ellipticity ϕ^H at H_s [Fig. 9a(a)], and therefore also the calculated values of the tilting angle [Fig. 9a(b)]. For uncovered part of the Fe(13 ML)/Ag(116) film the ellipticity ϕ^H measured at the $\alpha-$ and $\alpha+$ geometries is larger and smaller, respectively, than ϕ^H at the $\alpha^\parallel$ configuration. This corresponds to the orientation of the magnetization with the tilting angle $\delta = -3°$. After deposition of barely 1 ML of Au, the relation of the Kerr ellipticity at $\alpha-$ and $\alpha+$ with respect to $\alpha^\parallel$ is just opposite (i.e., ϕ^H at α^+ is larger than at $\alpha^\parallel$, while ϕ^H at $\alpha-$ is smaller than at $\alpha^\parallel$). It means that the magnetization, initially tilted by $\delta = -3°$, rotates upon covering with Au and becomes tilted by about $\delta = +3°$. The tilting angle value is nearly constant with further increase of Au thickness and starts to decrease gradually only above 8 ML of Au. The fact that Kerr ellipticity at $\alpha^\parallel$ is independent of Au thickness confirms that the observed change of the Kerr ellipticity at α^+ and

$\alpha-$ is not related to any magneto-optical effects. At 5 K (not shown), the dependence of the tilting angle looks qualitatively similar and no indication of the oscillatory behavior as a function of Au thickness is found neither for ϕ^H at H_s nor δ.

In order to explain theoretically the changes of the tilting angle with the increasing Au coverage we start with the values of K_s and k_{sp} fitted for the uncovered Fe(13 ML) film and the film covered with 15 ML of Au. We also assume that the anisotropy constants change with increasing Au thickness N_{Au} only in the range from 0 to 2 ML of Au and this dependence is linear, whereas for the Au overlayer thicker than 2 ML the constants K_s and k_{sp} are constant and equal to their fitted values at $N_{Au} = 15$ ML. This assumption is supported by the previous experimental finding by Hicken et al[36] that the anisotropy K_s of the Ag/Fe(6 ML)(001) film decreases almost linearly with the Ag overlayer thickness N_{Ag} if it is less than 2 ML and rapidly saturates at $N_{Ag} = 3$ ML. The assumed dependences of K_s and k_{sp} versus N_{Au} [Fig. 9a(c)] readily give the variation of δ with N_{Au} similar to the experimental dependence of the tilting angle which changes most significantly in the Au thickness range of 0 to 2 ML [Fig. 9a(d)]. One can notice however the difference of around 3 degrees between the experiment and theory for the uncovered Fe film (Au = 0 ML). This discrepancy is due to small deviations in the tilting angle values between different samples. By growing several test samples with uniform Fe thicknesses we have confirmed that even in the case of nominally homogenous substrate (as confirmed by Low Energy Electron Diffraction (LEED) and Scanning Tunneling Microscopy (STM)), there are always tiny differences in the magnetic anisotropy (and therefore the tilting angle) at different positions of the sample/crystal. In consequence, for the Au wedge sample shown in Fig. 9a(b), the value of the tilting angle for uncovered Fe film ($\delta = -3°$) is slightly different than in the case of Fe wedge sample from Fig. 6(b) (where for 13 ML thick Fe film $\delta = -1°$). The theoretical dependence reflects therefore what one would expect from Au wedge sample grown on perfectly homogenous Fe/Ag(116) surface.

The question remains whether the observed abrupt changes of the magnetization orientation upon submonolayer Au coverage depend on the Fe film thickness. In particular, one should note that in the case of 13 ML thick Fe film, the easy magnetization axis is oriented along the steps and therefore, the Kerr ellipticities ϕ^H at H_s as well as the tilting angle shown in Fig. 9a were obtained from the split hysteresis loops, i.e., correspond to the behavior of the intermediate axis, not the easy axis. To confirm the effect of Au on thinner Fe film, with canted magnetization, we report the results of SPLEEM experiment at zero magnetic field for the 4.5 ML thick Fe film as a function of Au coverage. The magnetic asymmetry, shown in Fig. 10(a) for three mutually perpendicular directions, provides information on how the easy direction of magnetization varies with the Au overlayer thick-
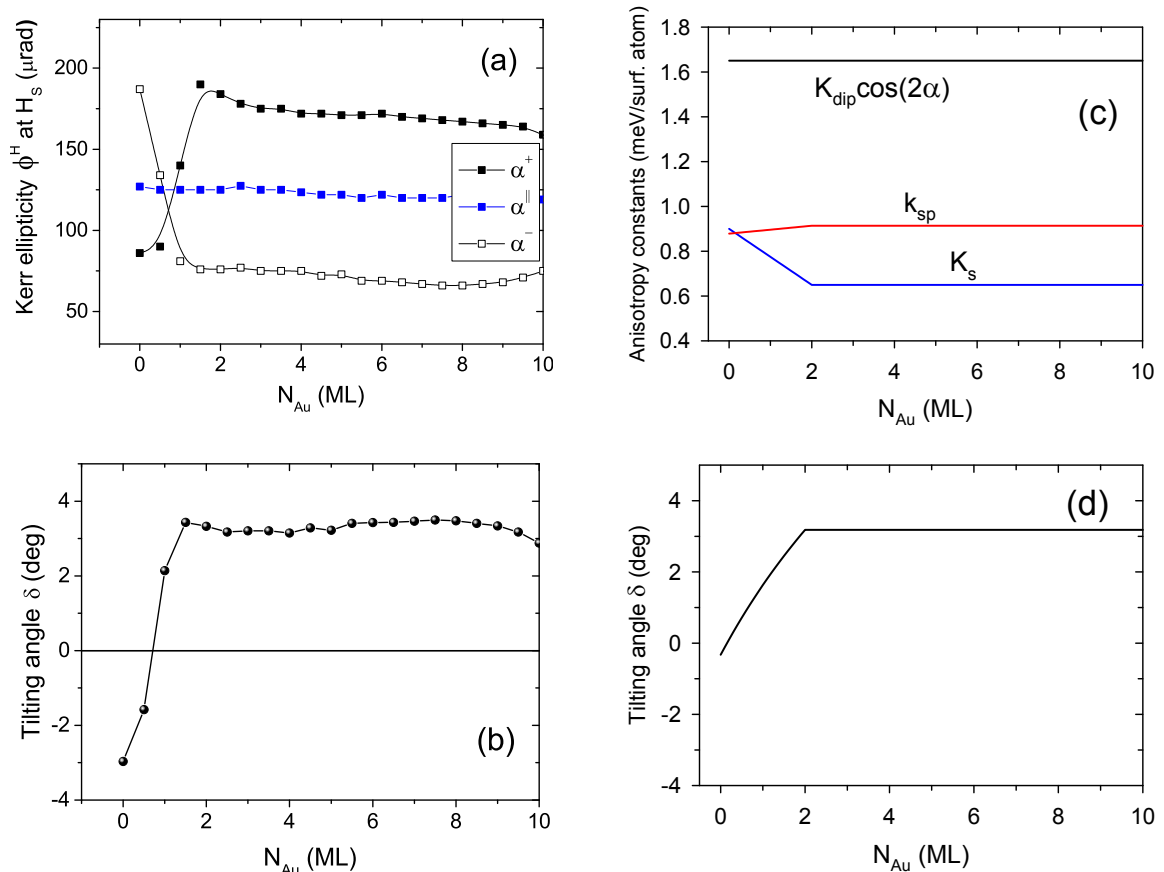
FIG. 9: (a) The dependence of (a) Kerr ellipticity ϕ^H at H_s and (b) the corresponding tilting angle δ (squares) as a function of thickness of the Au overlayer deposited on top of Fe(13 ML)/Ag(116) compared with (c) the model anisotropy constants and (d) fitted with them tilting angle δ.

ness. It is observed that the magnetization for the uncovered Fe(4.5 ML) films ($N_{Au} = 0$ ML) is canted within the plane perpendicular to the steps with the tilting angle of around $\delta = -73°$, which agrees with the MOKE results. Already 0.8 ML of Au causes dramatic changes in the domain structure and magnetic contrast is visible solely in the sample plane, with a strong contrast parallel to the step edges and hardly noticeable contrast perpendicular to the step edges. The magnetization remains oriented along the steps until the amount of deposited Au equals to 1.3 ML, where one can observe the magnetic contrast in both in-plane directions: parallel and perpendicular to the steps; state of coexisting phases is observed with adjacent domains oriented parallel and perpendicular to the steps. With further deposition of Au, the magnetization reorients fully towards perpendicular to the step edges direction (1.45 ML of Au) and no contrast along the step edges is visible.

To understand this variation of the easy magnetization direction we assume that all three MCA anisotropy constants K_s, k_{sp} and K_u change linearly with the Au overlayer thickness in the range from $N_{Au} = 0$ ML to

$N_{Au} = 2$ ML and are thickness-independent for thicker Au overlayers; see Fig. 10(b). We again take the boundary values of K_s and k_{sp} at $N_{Au} = 0$ and 2 ML from the previous fits for the uncovered and Au-covered Fe films (the anisotropy constants for $N_{Au} = 2$ ML are assumed to be the same as for $N_{Au} = 15$ ML). Then, also by taking suitable boundary values of K_u at $N_{Au} = 0$ and 2 ML, we find that, in some intermediate range of the Au thickness from 0.7 to 1.3 ML, the film energy for the magnetization parallel to the steps $E_{||} = E(\theta = 90°, \varphi = 90°)$ becomes lower than the minimum energy for magnetization perpendicular to the steps $E_{\perp}^{(min)} = E_{\perp}(\theta'_0)$, in a good agreement with the SPLEEM experiment; see Fig. 10(c).

This particular switching of the easy axis is possible because the difference of the two relevant energies, $\Delta E = E_{\perp}^{(min)} - E_{||}$, comprises two terms: $\Delta E_1 = (1/2)(K_{dip} - K_s - K_{eff,\perp})$, which grows with the Au thickness for the Au-covered Fe(4.5 ML) film, and $\Delta E_2 = K_u$, which decreases linearly with N_{Au}. The first term, which is present even for vanishing uniaxial anisotropy K_u within the terrace plane, results from the interplay of the three anisotropy constants K_{dip}, K_s, k_{sp} and its depen-
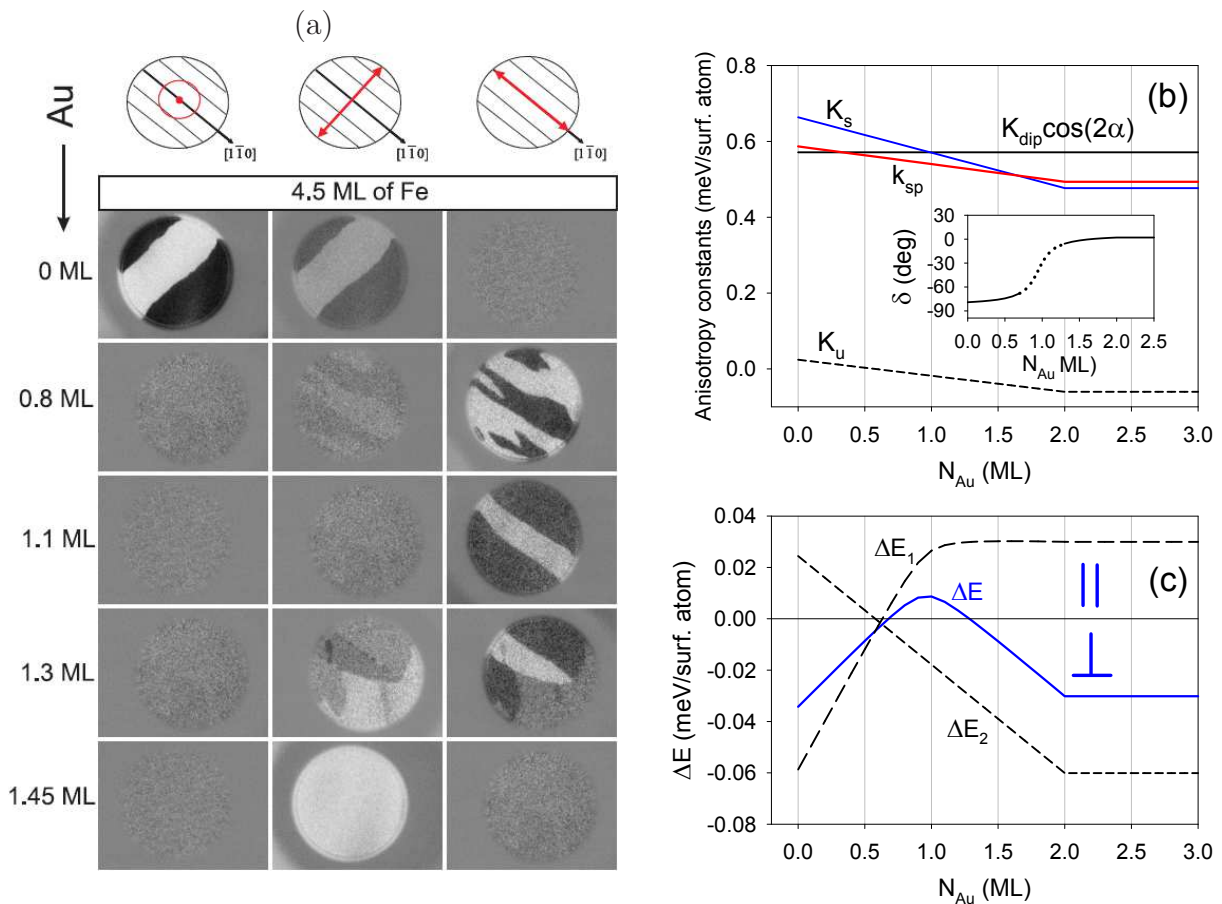
FIG. 10: (a) SPLEEM images with varying thickness of Au film grown on Fe(4.5 ML)/Ag(116) obtained at 130 K. Grey level, with respect to the background corresponding to zero magnetic contrast, represents orientation of magnetization with regard to the polarization of the incident electron beam (light and dark areas correspond to parallel and antiparallel orientations, respectively). Polarization direction of the incident beam is indicated on the top of the image columns. The f 12 μm in diameter; (b) the anisotropy constants (fitted as described in text); (c) the energy difference $\Delta E = E_\perp^{(\min)} - E_{||}$ (and its components ΔE_1 and ΔE_2) between the states with magnetization perpendicular and parallel to the steps. The tilting angle (insert in panel (b)) is found for the orientation perpendicular the steps (spontaneous or forced within the model) and marked with the solid line if $\Delta E < 0$ and with the dotted line if $\Delta E > 0$.

dence of these constants is nonlinear. The term is found to change sign from negative to positive, thus favouring switching the magnetization direction from perpendicular to parallel to the steps, while the tilting angle is still large ($\delta \approx 60°$ in the case shown in Fig. 10(b)). However, the presence of the second term can significantly change the favoured orientation of magnetization. In particular, it can keep the magnetization perpendicular to the steps even when the tilting angle is very small which is the case for the considered Fe(4.5 ML) film covered with a Au layer of the thickness of 1.45 ML and larger, like 15 ML (see Fig. 7). For this film, the superposition of the two terms of the ΔE has a maximum at $N_{Au} = 0.95$ ML, so that it is positive for $0.7\,\text{ML} \leq N_{Au} \leq 1.3$ ML and negative outside this thickness interval which corresponds to the observed sequence of switching the easy axis orientation with respect to the direction of the step

edges when the Au thickness increases. This agreement with the experimental results confirms the need for inclusion of the finite anisotropy constant K_u in the applied theoretical model of the magnetic anisotropy for cubic films on vicinal substrate surface though K_u has been claimed to be negligible for the bcc Fe films based on the Neel model[18,50].

VI. CONCLUSIONS

The results of this work demonstrate that well defined canted magnetization can be achieved without application of an external field. By taking advantage of broken symmetry of a vicinal substrate, we show that magnetic anisotropy of Fe films grown on the Ag(116) surface results in the canted magnetization with its azimuthal

orientation locked within the plane perpendicular to the step edges. The value of the tilting angle can be probed by longitudinal MOKE and precisely tuned by changing the thickness of Fe film and Au overlayer. This is possible thanks to continuous rotation of magnetization during the SRT from out-of-plane to in-plane direction with increasing thickness of Fe and the fact that the direction of magnetization rotation can be reversed by covering Fe films with Au layers. The change of the Fe magnetization direction takes place for the sub-monolayer Au coverage, up to 2 ML of Au. At low temperatures, QWS formed within Fe films come into play and contribute to the magnetocrystalline anisotropy, resulting in periodic modulations of the tilting angle, which substantially affects the magnetization rotation associated with the SRT. Employing all these mechanisms to modify the magnetic anisotropy of the Fe film allow for subtle adjustments of the tilting angle and virtually any magnetization orientation within the plane perpendicular to the step edges can be achieved in a reproducible manner.

The analysis of the proposed theoretical model reveals that the ferromagnetic system grown on vicinal surface can only be fully described if two additional, step-induced, anisotropy constants are included in the magnetic anisotropy energy of the film. The model reproduces the experimental findings and predicts that the tilting of magnetization results from the superposition of the three uniaxial magnetic anisotropies acting within the vertical plane perpendicular to the step edges. The magnetization tilting observed for the films on stepped substrate is not due the competition between the effective uniaxial anisotropy (with an easy axis perpendicular or parallel to the film surface) and the bulk anisotropy as it is the case for some films on atomically flat substrates[34,35]. Instead, it arises due to the fact that for films on vicinal substrates the easy axes of the shape and MCA perpendicular anisotropies are not perpendicular to each other since they are oriented perpendicularly to the sample surface and the terrace planes,respectively. As a result, SRT takes place over a thickness interval of around 3 ML, several times wider than for films on flat substrates. The tilting angle is significantly affected also by the step-induced anisotropy term with the easy axis oriented at $45°$ or $-45°$ to the terrace plane. The presence of this term is crucial for explaining the reversed rotation of magnetization upon covering the stepped Fe films by Au.

The presented methods allow for fine engineering of canted magnetization state and can be beneficial for control of the magnetization direction via voltage or optical pulses since tilted magnetization provides an additional torque and reduces the external energy required to switch the magnetization.

VII. ACKNOWLEDGMENTS

[1] F. D. Natterer, K. Yang, W. Paul, P. Willke, T. Choi, T. Greber, A. J. Heinrich, and C. P. Lutz, Nature **543**, 226 (2017), URL http://dx.doi.org/10.1038/nature21371.

[2] A. Stupakiewicz, K. Szerenos, D. Afanasiev, A. Kirilyuk, and A. V. Kimel, Nature **542**, 71 (2017), ISSN 0028-0836, URL http://dx.doi.org/10.1038/nature20807.

[3] P. Wadley, B. Howells, J. Železný, C. Andrews, V. Hills, R. P. Campion, V. Novák, K. Olejník, F. Maccherozzi, S. S. Dhesi, et al., Science **351**, 587 (2016), ISSN 0036-8075, http://science.sciencemag.org/content/351/6273/587.full.pdf, URL http://science.sciencemag.org/content/351/6273/587.

[4] W.-G. Wang, M. Li, S. Hageman, and C. L. Chien, Nat Mater **11**, 64 (2012), ISSN 1476-1122, URL http://dx.doi.org/10.1038/nmat3171.

[5] Y. Shiota, T. Nozaki, F. Bonell, S. Murakami, T. Shinjo, and Y. Suzuki, Nat Mater **11**, 39 (2012), ISSN 1476-1122, URL http://dx.doi.org/10.1038/nmat3172.

[6] G. Woltersdorf and C. H. Back, PRL **99**, 227207 (2007), URL https://link.aps.org/doi/10.1103/PhysRevLett.99.227207.

[7] C.-H. Lambert, S. Mangin, B. S. D. C. S. Varaprasad, Y. K. Takahashi, M. Hehn, M. Cinchetti, G. Malinowski, K. Hono, Y. Fainman, M. Aeschlimann, et al., Science **345**, 1337 (2014), ISSN 0036-8075, http://science.sciencemag.org/content/345/6202/1337.full.pdf, URL http://science.sciencemag.org/content/345/6202/1337.

[8] A. J. Schellekens, K. C. Kuiper, R. R. J. C. de Wit, and B. Koopmans, Nature Communications **5**, 4333 (2014), URL http://dx.doi.org/10.1038/ncomms5333.

[9] L. R. Shelford, Y. Liu, U. Al-Jarah, P. A. J. de Groot, G. J. Bowden, R. C. C. Ward, and R. J. Hicken, Phys. Rev. Lett. **113**, 067601 (2014), URL https://link.aps.org/doi/10.1103/PhysRevLett.113.067601.

[10] M. van Kampen, C. Jozsa, J. T. Kohlhepp, P. LeClair, L. Lagae, W. J. M. de Jonge, and B. Koopmans, Phys. Rev. Lett. **88**, 227201 (2002), URL https://link.aps.org/doi/10.1103/PhysRevLett.88.227201.

[11] F. Yildiz, M. Przybylski, and J. Kirschner, Phys. Rev. Lett. **103**, 147203 (2009), URL https://link.aps.org/doi/10.1103/PhysRevLett.103.147203.

[12] M. van Kampen, B. Koopmans, J. T. Kohlhepp, and W. J. M. de Jonge, Journal of Magnetism and Magnetic Materials **240**, 291 (2002), ISSN 0304-8853, URL http://www.sciencedirect.com/science/article/pii/S0304885301007818.

[13] C. Klein, R. Ramchal, A. K. Schmid, and M. Farle, Phys. Rev. B **75**, 193405 (2007), URL http://link.aps.org/doi/10.1103/PhysRevB.75.193405.

[14] S. S. Dhesi, H. A. Dürr, and G. v. d. Laan, Phys. Rev. B **59**, 8408 (1999), URL http://link.aps.org/doi/10.1103/PhysRevB.59.8408.

[15] A. Stupakiewicz, A. Maziewski, K. Matlak, N. Spiridis, M. Slezak, T. Slezak, M. Zajac, and J. Korecki, Phys. Rev. Lett. **101**, 217202 (2008), URL http://link.aps.

[16] org/doi/10.1103/PhysRevLett.101.217202.
M. Dąbrowski, M. Cinal, M. Przybylski, G. Chen, A. T. N. Diaye, A. K. Schmid, and J. Kirschner, Phys. Rev. B **93**, 064414 (2016).

[17] J. Li, M. Przybylski, Y. He, and Y. Z. Wu, Phys. Rev. B **82**, 214406 (2010), URL http://link.aps.org/doi/10.1103/PhysRevB.82.214406.

[18] R. K. Kawakami, E. J. Escorcia-Aparicio, and Z. Q. Qiu, Phys. Rev. Lett. **77**, 2570 (1996), URL http://link.aps.org/doi/10.1103/PhysRevLett.77.2570.

[19] J. Li, M. Przybylski, F. Yildiz, X. D. Ma, and Y. Z. Wu, Phys. Rev. Lett. **102**, 207206 (2009), URL http://link.aps.org/doi/10.1103/PhysRevLett.102.207206.

[20] U. Bauer, M. Dąbrowski, M. Przybylski, and J. Kirschner, Phys. Rev. B **84**, 144433 (2011), URL http://link.aps.org/doi/10.1103/PhysRevB.84.144433.

[21] M. Dąbrowski, T. Peixoto, M. Pazgan, A. Winkelmann, M. Cinal, T. Nakagawa, Y. Takagi, T. Yokoyama, F. Bisio, U. Bauer, et al., Phys. Rev. Lett. **113**, 067203 (2014), URL http://link.aps.org/doi/10.1103/PhysRevLett.113.067203.

[22] S. Manna, P. L. Gastelois, M. Dąbrowski, P. Kuswik, M. Cinal, M. Przybylski, and J. Kirschner, Phys. Rev. B **87**, 134401 (2013), URL http://link.aps.org/doi/10.1103/PhysRevB.87.134401.

[23] D. E. Bürgler, C. M. Schmidt, D. M. Schaller, F. Meisinger, R. Hofer, and H.-J. Güntherodt, Phys. Rev. B **56**, 4149 (1997), URL http://link.aps.org/doi/10.1103/PhysRevB.56.4149.

[24] K. Grzelakowski and E. Bauer, Rev. Sci. Instrum. **67**, 742 (1996), URL http://dx.doi.org/10.1063/1.1146802.

[25] N. Rougemaillea and A. K. Schmid, The European Physical Journal - Applied Physics **50**, 20101 (2010), URL http://www.epjap.org/10.1051/epjap/2010048.

[26] M. S. Altman, Journal of Physics: Condensed Matter **22**, 084017 (2010), ISSN 0953-8984, URL http://stacks.iop.org/0953-8984/22/i=8/a=084017.

[27] Y. Z. Wu, C. Won, H. W. Zhao, and Z. Q. Qiu, Phys. Rev. B **67**, 094409 (2003), URL http://link.aps.org/doi/10.1103/PhysRevB.67.094409.

[28] N. Mikuszeit, S. Pütter, and H. Oepen, Journal of Magnetism and Magnetic Materials **268**, 340 (2004), ISSN 0304-8853, URL http://www.sciencedirect.com/science/article/pii/S0304885303005456.

[29] T. Yokoyama, T. Nakagawa, and Y. Takagi, International Reviews in Physical Chemistry **27**, 449 (2008), ISSN 0144235X, URL http://search.ebscohost.com/login.aspx?direct=true&db=aph&AN=33193484&site=ehost-live&scope=site.

[30] M. Cinal, D. M. Edwards, and J. Mathon, Phys. Rev. B **50**, 3754 (1994), URL http://link.aps.org/doi/10.1103/PhysRevB.50.3754.

[31] T. Leeb, M. Brockmann, F. Bensch, S. Miethaner, and G. Bayreuther, J. Appl. Phys. **85**, 4964 (1999), URL http://dx.doi.org/10.1063/1.370059.

[32] Z. Celinski and B. B. Heinrich, J. Appl. Phys. **70**, 5935 (1991).

[33] B. Heinrich and J. Cochran, Advances in Physics **42**, 523 (1993), ISSN 0001-8732, URL http://dx.doi.org/10.1080/00018739300101524.

[34] Y. Millev and J. Kirschner, Phys. Rev. B **54**, 4137 (1996), URL http://link.aps.org/doi/10.1103/PhysRevB.54.4137.

[35] D. Stickler, R. Frömter, H. Stillrich, C. Menk, H. P. Oepen, C. Gutt, S. Streit-Nierobisch, L.-M. Stadler, G. Grübel, C. Tieg, et al., Phys. Rev. B **84**, 104412 (2011), URL http://link.aps.org/doi/10.1103/PhysRevB.84.104412.

[36] R. J. Hicken, S. J. Gray, A. Ercole, C. Daboo, D. J. Freeland, E. Gu, E. Ahmad, and J. A. C. Bland, Phys. Rev. B **55**, 5898 (1997), URL http://link.aps.org/doi/10.1103/PhysRevB.55.5898.

[37] M. Cinal (2018), unpublished.

[38] Z. Q. Qiu and S. D. Bader, Rev. Sci. Instrum. **71**, 1243 (2000), URL http://dx.doi.org/10.1063/1.1150496.

[39] P. B. Johnson and R. W. Christy, Phys. Rev. B **6**, 4370 (1972), URL http://link.aps.org/doi/10.1103/PhysRevB.6.4370.

[40] P. B. Johnson and R. W. Christy, Phys. Rev. B **9**, 5056 (1974), URL http://link.aps.org/doi/10.1103/PhysRevB.9.5056.

[41] J. Zak, E. R. Moog, C. Liu, and S. D. Bader, Phys. Rev. B **43**, 6423 (1991), URL http://link.aps.org/doi/10.1103/PhysRevB.43.6423.

[42] W. Geerts, Y. Suzuki, T. Katayama, K. Tanaka, K. Ando, and S. Yoshida, Phys. Rev. B **50**, 12581 (1994), URL http://link.aps.org/doi/10.1103/PhysRevB.50.12581.

[43] Y. Suzuki, T. Katayama, P. Bruno, S. Yuasa, and E. Tamura, Phys. Rev. Lett. **80**, 5200 (1998), URL http://link.aps.org/doi/10.1103/PhysRevLett.80.5200.

[44] B. Heinrich, Z. Celinski, J. F. Cochran, A. S. Arrott, and K. Myrtle, J. Appl. Phys. **70**, 5769 (1991), URL http://dx.doi.org/10.1063/1.350156.

[45] C. M., S. M., C. A., and M. L., Journal of Electron Spectroscopy and Related Phenomena **76**, 471 (1995).

[46] S. Terreni, A. Cossaro, G. Gonella, L. Mattera, L. Duo, F. Ciccacci, D. Cvetko, L. Floreano, A. Morgante, A. Verdini, et al., Phys. Rev. B **70**, 115420 (2004), URL http://link.aps.org/doi/10.1103/PhysRevB.70.115420.

[47] J. Li, G. Chen, Y. Z. Wu, E. Rotenberg, and M. Przybylski, Magnetics, IEEE Transactions on **47**, 1603 (2011), ISSN 0018-9464.

[48] M. Przybylski, M. Dąbrowski, U. Bauer, M. Cinal, and J. Kirschner, J. Appl. Phys. **111**, 07C102 (2012), URL http://dx.doi.org/10.1063/1.3670498.

[49] A. Hahlin, C. Andersson, J. H. Dunn, B. Sanyal, O. Karis, and D. Arvanitis, Phys. Rev. B **73**, 134423 (2006), URL http://link.aps.org/doi/10.1103/PhysRevB.73.134423.

[50] R. K. Kawakami, E. Rotenberg, E. J. Escorcia-Aparicio, H. J. Choi, T. R. Cummins, J. G. Tobin, N. V. Smith, and Z. Q. Qiu, Phys. Rev. Lett. **80**, 1754 (1998), URL http://link.aps.org/doi/10.1103/PhysRevLett.80.1754.